Available online at www.sciencedirect.com
ScienceDirect
Physica D 237 (2008) 699–720
PHYSICA D
www.elsevier.com/locate/physd

Minimal mechanisms for school formation in self-propelled particles

Yue-Xian Li*, Ryan Lukeman, Leah Edelstein-Keshet

Department of Mathematics, University of British Columbia, Vancouver, BC, Canada V6T 1Z2

Received 13 March 2007; received in revised form 28 September 2007; accepted 19 October 2007
Available online 25 October 2007

Communicated by H. Levine

Abstract

In the context of social organisms, a *school* refers to a cohesive group of organisms that share a common speed and direction of motion, as well as a common axis of body alignment or polarization. Schools are also noted for the relatively fixed nearest-neighbour distances between individuals. The rules of interaction that lead to the formation and maintenance of a school structure have been explored experimentally, analytically, and by simulation. Interest in biological examples, and non-biological "self-propelled particles" such as robots, vehicles, or autonomous agents leads to the question of what are the simplest possible sets of rules that can assure the formation and the stability of the "perfect school": an aggregate in which the nearest-neighbour distances and speeds are identical.

Here we explore mechanisms that lead to a perfect school structure in one and two dimensions. We consider distance-detection as well as velocity-detection between the interacting pairs of self-propelled particles. We construct interaction forces and formulate schooling equations. In the simplest cases, these equations have analytic solutions. In many cases, the stability of the perfect school can be explored. We then investigate how these structures form and evolve over time from various initial configurations using simulations. We study the relationship between the assumed interaction forces and the school patterns that emerge. While true biological schools are far from perfect, the insights gained from this investigation can help to understand some properties of real schools, and to suggest the appropriate properties of artificial schools where coordinated motion is desired.

Keywords: Social aggregation; Schooling behaviour

1. Introduction

A fundamental problem in biology is how behaviour and interactions at the level of the individual impact the emergent behaviour at the level of the group as a whole. In this paper, we examine the connection between individual behaviour and group properties within the context of social organisms that form a school or a flock. We ask how the parameters associated with each individual, together with the effective forces that represent their mutual interactions influence the existence of a school, its geometry, the speed and direction of movement, as well as the stability of the school structure.

Our perspective in this paper is based on the Lagrangian viewpoint, that is, we follow individual particles, rather than densities of organisms. We formulate equations of motion based on the Newtonian approach, i.e. describing changes in the velocities and positions of the particles under forces of propulsion and interaction. Such an approach leads to a generalized system of ordinary differential equations

$$\dot{\vec{x}}_i = \vec{v}_i, \tag{1}$$

$$\dot{\vec{v}}_i = \vec{f}_a + \vec{f}_i, \tag{2}$$

* Corresponding author. Tel.: +1 604 822 6225.
E-mail address: yxli@math.ubc.ca (Y.-X. Li).

0167-2789/$ - see front matter © 2007 Elsevier B.V. All rights reserved.
doi:10.1016/j.physd.2007.10.009

where $\dot{\vec{x}} \equiv d\vec{x}/dt$ denotes a derivative with respect to time. Here, we classified all forces into two general categories: $\vec{f}_a$ that is generated autonomously by each individual without the influence of other individuals and $\vec{f}_i$ that is generated due to the interaction with others. Depending on the specific choice of these forces, the model can have very different properties. For example, in [4,7, 12–14], $\vec{f}_a = (\alpha - \beta|\vec{v}_i|^2)\vec{v}_i$ was studied. This model was originally obtained by minimizing the specific energy cost of a swimming fish [26]. In [8], $\vec{f}_a = -\beta\vec{v}_i$ which is simply a drag force that helps to stabilize the motion of a particle. In both of these models, the movement of an individual is purposeless in the absence of the interaction with other particles. It either stays motionless or keeps moving at a constant speed along its initial direction of motion. In the present study however, there is some preferred direction, and each individual knows where to go and whether it is at a leading position in the group.

The interaction force $\vec{f}_i$ that is directly responsible for many important characteristics of the emergent aggregate pattern plays a key role in defining a distinct model. Pairwise interaction is the most commonly studied force, although in [8], a localized mean field interaction was used to describe the influence of nearest neighbours on the movement of a particle. Interactions with infinite range and all-to-all coupling have been considered in most studies cited above as well as the study of non-Newtonian particles moving in viscous media [11]. An important question considered in these studies is how the specific features of the aggregate change as the number of particles is increased. Whether the nearest-neighbour distance (NND) collapses to zero in the limit of an infinitely large group of particles has been shown to influence strongly the possible school patterns that can occur in the system [11, 4,7]. In the present study, our focus is very different from these studies. We are not concerned with the effects of an infinite size of the group but rather focus on groups with finite number of particles and with short-range interactions. In most cases, we only consider nearest-neighbour interactions. Our main goals are to find analytic insights, based on simplifications and assumptions that render the problem amenable to analysis. These insights allow us to pinpoint the minimal mechanism that determines each specific feature of a school pattern. This approach is also different from a number of other studies in which numerical insights were the main focus [1,5,6,17,20,2,3,25]. In order to arrive at analytic results, we consider the classes of special solutions that we refer to as *perfect schools*. These are configurations of particles in which the spacing is constant and identical, and where individuals in the group move at a constant speed. We further subdivide perfect schools into those in which individuals share a common heading, and those in which they do not. In this paper, we are primarily concerned with the former. This is the Lagrangian analogue to motion as a traveling wave with uniform interior density.

It is well-known that aggregates occur if the particles mutually attract at long distances and repel at short distances. When the interaction is all-to-all, the NND can approach zero as the size of the group increases depending on whether the pairwise interaction satisfies certain conditions [11,4,7]. A large number of possible transient and static patterns can occur in particles that interact with each other in such a way, and it is beyond the scope of this paper (and likely impossible) to predict all possible patterns. In this paper, we focus mainly on regular arrays, both in 1D and 2D, that are reached after the transient state is over. Our approach is to exploit the simplicity of these regular schools in an attempt to address the following questions analytically: (i) Under what conditions on the school forces do such perfect schools occur (existence)? (ii) Given their existence, what further conditions guarantee that these patterns are not destroyed by random perturbations (stability)? While real schools and flocks are much more plastic and irregular, focusing on these patterns leads to clear-cut results that can be derived analytically.

The relative simplicity of our model and the precise definition of these special solutions allow us to reach several new conclusions that are difficult to obtain by simulations alone. We will show that by looking for perfect school solutions, we arrive at conditions linking self-propulsion forces with interaction forces evaluated at the NND. Stability depends on the slope of the interaction force as a function of NND. The structure of the interaction matrix that determines how many neighbours interact with each individual is crucial for achieving explicit stability analysis. At the same time, in order to extend our results to cases that are too challenging to analyze fully, or to more complex cases, we complement our study with numerical simulations.

Our main goal in this paper is to understand which factors lead to which of the properties of a group. As will be shown, the questions posed above can be answered conclusively only when the analytical solutions of the schools and explicit expressions for determining their stability can be achieved. Many realistic school structures observed in nature are irregular under the influence of noise from various sources. The range of structures that we explore, however, belongs to a class of simple and regular patterns that allow us to achieve analytical results and predictions. These structures are often observed in nature (albeit more irregular), and based on our theory presented in this paper, are the most likely realized patterns given simple rules of nearest-neighbour interaction.

The questions posed above can be answered conclusively in the case of the special solutions that form the class of interest. This would not be true if we were to consider all possible (dynamic and steady state) group configurations that satisfy our model equations. For this reason, we do not consider a variety of more complicated and more realistic group structures that occurs in nature. Nevertheless, the range of structures that we do explore is consistent with groups of autonomous robots, or formations of vehicles on a highway or in military environments, topics that have emerged as recent areas of application of such theory. Understanding the possible behaviour of such artificial autonomous self-propelled agents forms an additional motivation for this paper.

In Section 2, we introduce the basic assumptions of the model we use in this study and the differential equation system that describes the motion of the particles. In Section 3, we study schools in 1D space analytically and numerically. The simplicity of these school solutions allows us to develop a basic theoretical framework. We also introduce the concept of stressed and stress-free schools. In Section 4, a soldier formation solution in two dimensions has been studied analytically using a similar approach as in Section 2. Numerical simulations in 2D are then used to verify analytical results on soldier formations. In Section 5, we

discuss some numerical results that demonstrate the formation of other types of 2D arrays. Results are summarized and discussed in Section 6.

2. The model of interacting self-propelled particles

2.1. Assumptions and equations

The following basic assumptions apply to the schools that we study in this paper.

(A1) All particles are identical and obey the same set of rules.
(A2) Each particle is capable of sensing if it is located in the interior or at the edge (front/rear) of the school.
(A3) The force experienced by one particle from a given neighbour is composed of a distance-dependent term and a velocity-dependent term. Only pairwise interactions are considered.
(A4) The forces exerted by different neighbours are additive.
(A5) The magnitude of the forces between a pair of particles depends on the distance between the pair and their relative velocities.
(A6) The distance-dependent force between a pair is a vector parallel to the vector connecting the pair while the velocity-dependent force is parallel to the difference between the velocities of the pair.

Consider a group of n self-propelled particles, each identified by a subscript $i = 1, 2, \ldots, n$, with position and velocity denoted by $\vec{x}_i$ and $\vec{v}_i$, respectively. We assume that particles are polarized, that is, each has a front and a back. For simplicity, we assume that the body alignment of the ith particle is identical to its direction of motion, i.e. the direction of $\vec{v}_i$. The movement of the ith particle is governed by the classical Newton's Law of Motion which yields

$$\dot{\vec{x}}_i = \vec{v}_i, \tag{3}$$

$$\dot{\vec{v}}_i = \vec{a}_i - \gamma \vec{v}_i + \vec{f}_i, \tag{4}$$

where the mass of each individual is scaled so that $m_i = 1$ for all particles. $\vec{a}_i$ is an autonomous self-propulsion force generated by the ith particle which may depend on environmental influences and on the location of the particle in the school. This is the term that distinguishes this model different from some previously studied models [12,11,4,7]. The term $\gamma \vec{v}_i$ is a damping force with a constant drag coefficient γ (>0) which assures that the velocity is bounded. Eq. (4) implies that if a particle stops propelling, its velocity decays to zero at the rate γ. $\vec{f}_i$ is the interaction or schooling force that moves the ith particle relative to its neighbour(s). If one particle described by (3) and (4) is moving in D-dimensional space ($D = 1, 2, 3$), the number of first-order equations for each particle is $2D$. For a group of n such particles, there are $2Dn$ first-order equations.

In the following analysis, $\vec{a}_i$ is typically a constant vector which may be different for a leader, follower or individual in the tail (i.e., the last particle) of the group. Based on the model assumptions (A3)–(A6), the schooling force is given by

$$\vec{f}_i \equiv \vec{f}_i^{\,x} + \vec{f}_i^{\,v} = \sum_j g_\pm(|\vec{x}_{ji}|)\frac{\vec{x}_{ji}}{|\vec{x}_{ji}|} + \sum_j h_\pm(|\vec{v}_{ji}|)\frac{\vec{v}_{ji}}{|\vec{v}_{ji}|}, \tag{5}$$

where

$$\vec{x}_{ji} = \vec{x}_j - \vec{x}_i; \qquad \vec{v}_{ji} = \vec{v}_j - \vec{v}_i.$$

$\vec{f}_i^{\,x}$ and $\vec{f}_i^{\,v}$ are the position- and velocity-dependent forces, respectively. Index j sums over all the particles that influence the movement of particle i. g_+ and h_+ (g_- and h_-) are chosen when the influence comes from the front (behind), i.e. if $\vec{x}_{ji}\cdot\vec{v}_i > 0$ (<0). $g_+ \neq g_-$ and $h_+ \neq h_-$ imply that the forces from particles in front and those from particles behind are different or asymmetric. $g_\pm(x)$ are defined for $x \geq 0$, i.e., are functions of the absolute distance between two particles. To produce a nonzero spacing distance, $g_\pm(x)$ should typically be positive for large x and negative for small x, indicative of short-range repulsion and long-range attraction. This feature is universal in almost all models of aggregate formation. (See review of attraction–repulsion models in [11].) In most results that we studied in this paper, $g_\pm(x)$ possesses such a feature, unless specified otherwise. Furthermore, the forces that each particle can generate should be bounded.

Based on these definitions, $g_+(\cdot) > 0$ (<0) means that particle j which is in front of particle i exerts an attractive (repulsive) force on the latter; while $h_+(\cdot) > 0$ (<0) implies that the velocity-dependent force makes the velocity of particle i converge to (diverge from) that of particle j (see Fig. 1). Note that the position-dependent and velocity-dependent components of the schooling force can point to different directions and possess different magnitudes. All constants and functions that appear in (3)–(5) are model inputs that are assumed to be given.

Different choices of the functions $g_\pm$ and $h_\pm$ can generate large numbers of school formations that are qualitatively different. Further classification of the subtypes of these models is possible based on specific selection of these functions. We do not intend to take on such a task in this paper. However, examples that we present in the following sections clearly demonstrate the crucial importance of the form of these functions in determining the school patterns that emerge.

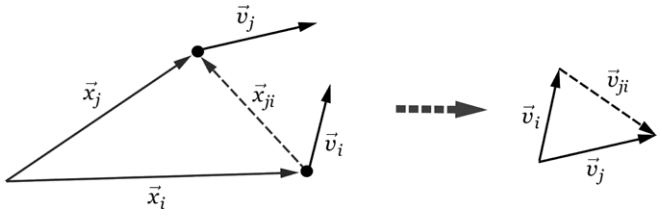

Fig. 1. A schematic diagram of model vectors in 2 dimensions.

Using the classical Newton's Law of Motion to describe a system of self-propelled particles is an approach adopted in numerous previous studies [8,15,16] although, as we shall discuss later, differences in the dynamics that govern the autonomous self-propulsion and in the range of pairwise interactions can lead to significant differences in the school patterns that can emerge.

2.2. Classification of schools

Having given the definition of perfect schools in Section 1, we note that such schools can be further divided into two types: those in which each individual has an identically constant direction, denoted as *Type I* schools, and those in which the individuals change direction in time, denoted as *Type II* schools. Type I schools are the main focus of this paper. Type II schools are typically more difficult to analyze. A good example is a mill formation, in which the particles rotate around an invariant circle (see, e.g., [10]). Here, headings are changing continuously as particles rotate, and each individual has a different heading at any given time. Other Type II schools include groups collectively performing a turning manoeuvre. Note that in both Types I and II perfect schools, the group moves collectively as a rigid body under transformation (e.g., translation, rotation, etc).

For a perfect school, we can define the *center of mass* and the *school velocity* by

$$\vec{X}(t) = \frac{1}{n}\sum_{i=1}^{n}\vec{x}_i(t), \qquad \vec{V}(t) = \frac{1}{n}\sum_{i=1}^{n}\vec{v}_i. \tag{6}$$

The combined autonomous self-propelling force and schooling force are:

$$\vec{A} = \frac{1}{n}\sum_{i=1}^{n}\vec{a}_i, \qquad \vec{F} = \frac{1}{n}\sum_{i=1}^{n}\vec{f}_i. \tag{7}$$

Using these definitions, we can write down the equations of motion of the school as a whole.

$$\dot{\vec{X}} = \vec{V}, \tag{8}$$

$$\dot{\vec{V}} = \vec{A} + \vec{F} - \gamma\vec{V}. \tag{9}$$

In the special case $\vec{v}_i = \vec{V}$, where $\vec{V}$ is a constant vector and identical for all i (i.e., a Type I school), the equations of motion for each individual must be identical to those of the whole school.

We distinguish between two types of individuals: those denoted as leaders, and their followers. In general, we define a *leader particle* as an individual that does not see any other particles in its frontal visual field, where the sign of $\vec{v}_i \cdot \vec{x}_{ji}$ distinguishes the frontal and rear visual fields. All others are denoted as followers. We associate distinct self-propelling forces $\vec{a}^l$ and $\vec{a}$ with the leaders and the followers respectively (where the superscripts are labels, not exponents). In 1D schools, we consider the special case of interactions both to the front and rear of an individual. In this case, we additionally distinguish between a *tail particle* (i.e., an individual that does not see any particles in its rear visual field) and other interior followers, and associate a distinct self-propelling force $\vec{a}^t$ with the tail particle.

In our model of school formation, we consider as inputs the leader and follower autonomous self-propulsions $\vec{a}^l$ and $\vec{a}$, and the interaction functions $g_\pm$ and $h_\pm$. Model outputs are the individual distance d between particles, the school velocity $\vec{v}$ and (where applicable) the autonomous self-propulsion of the tail a_t.

The perfect schools that we study in this paper are idealizations of some observed social aggregates in nature. Fish schools in the form of surface sheets or linear soldier formations are often encountered. Single-file trail following occurs in ants, caterpillars, as well as birds; linear and $\vee$-shaped flocks are observed in formations of many bird species.

The analytical methods we adopt here are very similar to those used in the study of synchronized clustered states in neuronal networks [9]. We substitute a specific school solution of interest into the system of nonlinear differential equations and determine the conditions for the existence of such a solution. Then, we introduce a small perturbation in the equations near this school solution and linearize the system. We find the eigenvalues of the linearized system, and we determine the conditions that make their real parts negative. We then verify these existence and stability conditions using numerical simulations of the system, and explore patterns that arise from arbitrary initial conditions.

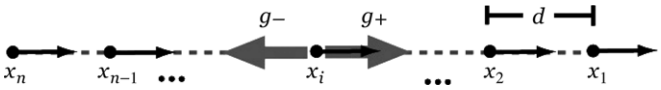

Fig. 2. A schematic diagram of particles in one dimension, showing our subscripting convention. Grey arrows indicate distance-dependent interaction forces.

3. Schools in 1D space

Aggregates of animals moving on a single trail are examples of schools in one-dimensional space (1D). Vehicles moving on a single-lane highway can form similar aggregates. Consider a group of n particles moving in 1D. The equations of motion are now reduced to the scalar equations:

$$\dot{x_i} = v_i, \tag{10}$$

$$\dot{v_i} = a_i - \gamma v_i + f_i, \tag{11}$$

where $i = 1, 2, \ldots, n$. For convenience, we associate the label 1 with the leading particle, and sequentially label the remaining $n-1$ particles (see Fig. 2). Then $a_1 \equiv a^l$ and $a_i \equiv a$ for $i = 2, \ldots, n-1$, and $a_n \equiv a^t$.

Once a perfect school in 1D is formed, only two quantities are required to completely characterize the school: its velocity, v, and nearest-neighbour distance, d. These will be determined by the choice of specific interaction forces and parameter values. According to Eq. (5), the schooling force is given by

$$f_i = \sum_j g_\pm(|x_{ji}|)\frac{x_{ji}}{|x_{ji}|} + \sum_j h_\pm(|v_{ji}|)\frac{v_{ji}}{|v_{ji}|}, \tag{12}$$

where $x_{ji} = x_j - x_i$ is the distance between the neighbours and $v_{ji} = v_j - v_i$ is the relative velocity of particles i and j, and the summation is over all particles that influence the movement of particle i.

We change into a coordinate system that is moving at the school speed v. Let p_i and q_i be the position and velocity of the ith particle in this moving coordinate. Using the relation $p_i = x_i - vt$ and $q_i = v_i - v$, we obtain the dynamic equations in the moving frame:

$$\dot{p_i} = q_i, \tag{13}$$

$$\dot{q_i} = a_i - \gamma(q_i + v) + f_i. \tag{14}$$

In the moving frame, a perfect school solution corresponds to a stationary distribution of the particles in space. Thus, every perfect school must be a steady-state solution of (13) and (14); i.e., $\dot{p_i} = 0$, $\dot{q_i} = 0$, for which

$$q_i = 0, \tag{15}$$

$$a_i - \gamma v + f_i = 0, \tag{16}$$

for all i. For such a steady state,

$$f_i = \sum_j g_\pm(|j-i|d)\,\mathrm{sgn}(j-i) + \sum_j h_\pm(0)0 = \sum_j g_\pm(|j-i|d)\,\mathrm{sgn}(j-i), \tag{17}$$

where j sums over all particles that influence particle i and where

$$\mathrm{sgn}(j-i) = \frac{j-i}{|j-i|}.$$

Eq. (17) implies that for a steady-state solution in which the interaction connections are fixed, all the schooling forces are functions of d only.

3.1. Schools formed by following one immediate neighbour

The simplest case of a perfect school in one dimension occurs when each particle follows only one nearest neighbour at constant distance d in front of it. Then the leader feels no schooling force, i.e., $f_1 = 0$, so $a^l - \gamma v = 0$ while all followers including the last particle experience the same schooling force $f_i = g_+(d)$. Because the tail particle interacts in the same way as the interior particles, we let $a = a_t$, so $a_n \equiv a$. Evaluating Eq. (16) at steady state for the leader gives $v = a^l/\gamma$. Substituting this expression for v into Eq. (16) and evaluating at steady state for a follower gives $g_+(d) = a^l - a$. The value of d is determined by the number of intersection points between the function $g_+(x)$ and the horizontal line at the value $a^l - a$. There could be zero, one, two, or more intersection points depending on the functional form of $g_+(x)$, implying that the number of school formations that exists could be zero, one or more. As we shall illustrate later, not all solutions are stable. The stability depends on the slope of $g_+(x)$ at each intersection point.

Note that if all particles have identical autonomous self-propulsion, i.e. $a_i = a$, then $f_i = g_+(d) = 0$ when the school is formed, implying that all schooling forces vanish at the steady-state perfect school. Only when the particles deviate from their 'preferred' positions in the school, the schooling forces would become nonzero. Then the effects of these forces bring the particles back to their correct positions (if stable) or amplify the deviation (if unstable). A school in which schooling forces vanish at steady state will be denoted as a *stress-free* school. However, if the leader has a distinct self-propulsion, i.e. $a^l \neq a$, then $f_i = a^l - a \neq 0$ which means that the schooling forces do not vanish when the school is formed. We shall call such a school a *stressed* school.

3.2. Schools formed by interactions with two nearest neighbours

Consider a 1D school with particles labeled as in Fig. 2, such that $a_1 = a^l$, $a_i = a$ for $i = 2, \ldots, n-1$ and $a_n = a^t$. Now, we assume that each particle interacts with its nearest neighbours ahead and behind it, giving the following interaction forces:

$$f_1 = -g_-(|x_2 - x_1|) + h_-(|v_2 - v_1|)\,\mathrm{sgn}(v_2 - v_1), \tag{18}$$

$$f_i = g_+(|x_{i-1} - x_i|) - g_-(|x_{i+1} - x_i|) + h_+(|v_{i-1} - v_i|)\,\mathrm{sgn}(v_{i-1} - v_i) + h_-(|v_{i+1} - v_i|)\,\mathrm{sgn}(v_{i+1} - v_i), \quad i = 2, \ldots, n-1, \tag{19}$$

$$f_n = g_+(|x_{n-1} - x_n|) + h_+(|v_{n-1} - v_n|)\,\mathrm{sgn}(v_{n-1} - v_n). \tag{20}$$

When a school is formed, $v_i = v$ and $x_{i-1} - x_i = d$ (and thus $x_{i+1} - x_i = -d$) for all i, which implies that

$$f_1 = -g_-(d), \tag{21}$$

$$f_i = g_+(d) - g_-(d), \quad (i = 2, \ldots, n-1), \tag{22}$$

$$f_n = g_+(d). \tag{23}$$

Next, we substitute these forces into the steady-state equation (14) which gives

$$\gamma v = a^l - g_-(d), \tag{24}$$

$$\gamma v = a + g_+(d) - g_-(d), \tag{25}$$

$$\gamma v = a^t + g_+(d), \tag{26}$$

where $a_n = a^t$ denotes the autonomous self-propulsion of the tail particle. Solving these equations for v, a^l, and a^t we obtain

$$v = \frac{1}{\gamma}[a^l + a^t - a], \tag{27}$$

$$a^l = a + g_+(d), \tag{28}$$

$$a^t = a - g_-(d), \tag{29}$$

which leads to the following conclusions:

1. The speed of the school depends explicitly only on the self-propulsion forces a^l, a^t and a and γ, among which a^l and a are parameters with fixed values. Eq. (28) determines the value of d as well as the number of possible school solutions based on the given form of $g_+(d)$. Once the value of d is determined, Eq. (29) determines the value of a^t, which is the self-propulsion force the tailing particle must adopt in order to keep up with the school.
2. Individuals at the front or rear of the group have fewer interactions. Thus, to keep a fixed nearest-neighbour distance, some compensation for missing forces is needed. Otherwise, it would be impossible to maintain a perfect school.

We note that in many biological examples, which deviate significantly from our perfect school assumptions, there is crowding at the edges of a herd or swarm. Examples of this type occur in herds of wildebeest shown in [19] and in locust hopper bands [24]. Both examples show a gradual increase of density of individuals towards a front edge, and sharp boundary at that edge.

In the case of interactions with both nearest neighbours, a stress-free steady-state solution implies that $g_+(d) = g_-(d) = 0$. From Eqs. (27)–(29), the stress-free condition implies that $a^t = a^l = a$, and $v = a/\gamma$ at steady state; that is, each individual must have the same autonomous self-propulsion, and the school velocity is dependent only on the common autonomous self-propulsion and the friction coefficient.

Alternatively, for a stressed solution with nearest-neighbour distance d and $v > 0$, (27)–(29) imply that

$$a^l > g_-(d). \tag{30}$$

The school velocity is given by $v = [a^l - g_-(d)]/\gamma$, and thus (30) assures that $v > 0$. Further, Eq. (30) means that the leading particle must generate a sufficiently large autonomous self-propelling force to overcome attraction (or effective drag) due to the particle behind it, while the difference between the two forces determines the school speed. Eq. (28) means that the difference

between a^l and a together with the functional form of $g_+(x)$ determines the number, and values of allowable group spacing d. For fixed a^l and a, the autonomous self-propulsion of the tail particle must be adjusted to satisfy Eq. (29). We note that a stressed school can occur even if a^l and a have different signs; i.e., if the self-propulsions of the leading particle and interior particles are in opposite directions. In this case, the schooling forces overpower the intrinsic motion of the interior particles. In this sense, interior individuals are all followers, with the tail particle a special type of follower whose autonomous self-propulsion is distinct from that of the other followers. We note that Eqs. (28) and (29) place a further restriction on $g_\pm(x)$: that $a^l - a \leq \max_x(g_+(x))$, and that $a - a^t \leq \max_x(g_-(x))$ to guarantee the existence of at least one perfect school solution.

As one example, suppose that $a = 0$ for all interior particles i.e., individuals base responses on interactions alone, instead of intrinsic autonomous forces. In such a school, to keep a nearest-neighbour distance d, $a^t = -g_-(d)$ for the tail particle. The spacing distance d is determined from (28), i.e., $a^l = g_+(d)$. Then for a monotonic increasing $g_+(x)$, increasing a^l results in a larger nearest-neighbour distance d. However, because steady-state velocity is $v = [a^l - g_-(d)]/\gamma$, increasing a^l does not necessarily increase v. Instead, Eq. (27) implies that

$$v = \frac{1}{\gamma}\left(g_+(d) - g_-(d)\right). \tag{31}$$

Eq. (31) illustrates the relationship between school velocity and spacing. Specifically, if the slope of $g_+(x) - g_-(x)$ is positive, the distance d between neighbours in the school increases as school velocity v increases. On the other hand, if the slope of $g_+(x) - g_-(x)$ is negative, d decreases as v increases. Examples of these two different cases are shown in Fig. 5. This result is immediately applicable to the experimental observations. For example, if the NND d increases as the school moves with a higher speed, there is reason to believe that the case in Fig. 5.a might be occurring. It is almost impossible to determine the functional form of $g_\pm(x)$ for realistic animals, but by observing the relationship between the changes in school speed and the NND, we can comment on the nature of the slope of $g_+(x) - g_-(x)$. Note that $a = 0$ is not required for this result; in the case $a \neq 0$, $v = a/\gamma + (1/\gamma)\left(g_+(d) - g_-(d)\right)$, which is identical to Eq. (31), except for a shift in velocity of a/γ.

3.3. Examples of some schooling forces

3.3.1. Distance-dependent forces

The theory developed so far applies to any functions $g_\pm(x)$, $h_\pm(x)$. However, requiring realistic schooling forces restricts our choice of functions. For distance-dependent forces, we take as a specific example Hill functions, i.e., saturating monotonic increasing functions of x:

$$g(x) = c\left[\frac{(1 + k^m/d_0^m)x^m}{x^m + k^m} - 1\right], \quad (m \geq 1), x \leq x_f. \tag{32}$$

$m > 0$ and $d_0 > 0$ represent the steepness and x-intercept of $g(x)$, respectively. Note that $g(0) = -c$ and $c[1 + k^m/d_0^m]$ are, respectively, the minimum and the saturation values of $g(x)$. Eq. (32) defines a four-parameter family of functions from which $g_+(x)$ and $g_-(x)$ might be chosen. A decay beyond some finite distance can represent a limited sensing range ($0 \leq x \leq x_f$) of the individuals. Fig. 3 shows a typical distance-dependent schooling force based on a Hill function. Other typical forces used include exponential forces of the form

$$g(x) = A\exp(-x/a) - R\exp(-x/r), \tag{33}$$

or inverse power forces

$$g(x) = \frac{A}{x^a} - \frac{R}{x^r},$$

where A, R, a, and r are parameters (see [11]).

3.3.2. Velocity-dependent forces

In one dimension, the velocity-dependent forces $h_\pm(v)$ have a simple interpretation. In this case, all individuals have the same absolute direction (though they may differ by a sign, depending on whether movement is along the axis in the positive or negative direction). Then the velocity-dependent force given by Eq. (12) summed over influencing neighbours,

$$\hat{h}_\pm(|v_{ji}|)\frac{v_{ji}}{|v_{ji}|},$$

can be represented as a single function of v_{ji}, since in 1D the direction term $v_{ji}/|v_{ji}|$ is simply $\mathrm{sgn}(v_{ji})$, i.e., ± 1. We thus define

$$\hat{h}_\pm(v) = h_\pm(|v|)\frac{v}{|v|},$$

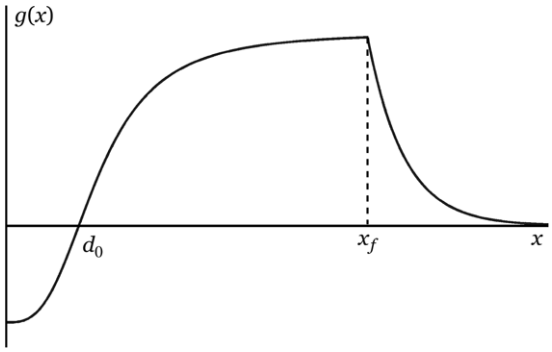

Fig. 3. An example of a distant-dependent force in the form of a Hill function with a decay past x_f, to depict a finite sensing range.

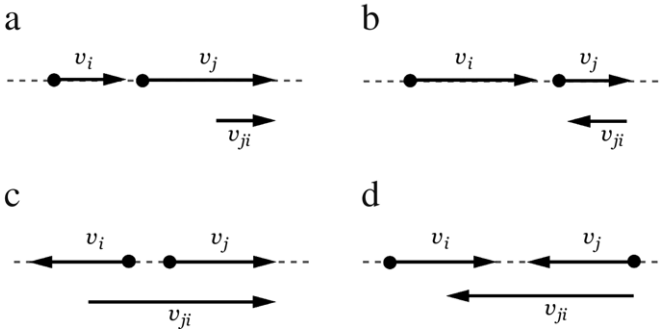

Fig. 4. Four cases of neighbour interaction: (a) neighbour j travels faster than i in the same direction, ($v_{ji} > 0$), (b) neighbour j travels slower than i in the same direction, ($v_{ji} < 0$), (c) neighbour j diverging from i, ($v_{ji} > 0$), (d) neighbour j converging to i, ($v_{ji} < 0$).

where $h(v)$ is defined for all $v \in \mathbf{R}$. There are a number of cases to consider when determining reasonable forms of $h(v)$. From Fig. 4, the influence of a neighbour j on the velocity v_i of individual i should cause acceleration when $v_{ji} > 0$, but deceleration when $v_{ji} < 0$. We assume that there is no influence when $v_i = v_j$, i.e., $h(0) = 0$. We will later show that under the assumption $h(0) = 0$, $h(v)$ has no effect on the existence of a perfect school solution. Thus, a reasonable form of $h(v)$ is a monotonically increasing function with $h(0) = 0$. This type of assumption is incorporated in models for swarming in 2D and 3D, discussed in [17,20,12,15,16] as "arrayal forces", since these forces act to array individuals in parallel. As an example, the function we use in this paper is

$$h(v) = C \tanh(v/\rho),$$

where $C > 0$ and ρ are parameters governing the amplitude and steepness of $h(v)$, respectively. If $\rho < 0$, $h(v)$ is monotonically decreasing; we include this generality, but we will later show that only the monotonically increasing case ($\rho > 0$ in this example) enhances stability of the perfect school solution. As in the distance-dependent functions, particular choices of parameters lead to different shapes of functions for $h_+(v)$ and $h_-(v)$. In [8], $h(v) = \alpha v$ ($\alpha > 0$ is a constant) in the case when only nearest-neighbour interactions are considered.

The number of reasonable choices of the functions $g_\pm(x)$ and $h_\pm(v)$ that yield qualitatively identical results as the expressions we adopted in this study is unlimited. Any information that leads extra restrictions of these functions would be valuable for making our choices more realistic.

3.4. The stability of a school solution

We next explore the stability of a 1D perfect school. To do so, we consider a perfect type I school, moving with speed v and nearest-neighbour distance d: $v_i^s = v$ and $x_i^s = x_1^0 + vt - (i-1)d$ (where x_1^0 is the position of the leading particle at $t = 0$). This corresponds to the steady-state solution $p_i^s = x_1^0 - (i-1)d$ and $q_i^s = 0$ in the moving-frame coordinates.

Using the moving-frame analogues of Eqs. (18)–(20) and (12), and the expression for v from Eq. (27) in Eqs. (13) and (14), we obtain the moving-frame equations of motion for nearest-neighbour interactions ahead and behind individuals:

$$\frac{\mathrm{d}p_i}{\mathrm{d}t} = q_i, \tag{34}$$

$$\frac{\mathrm{d}q_1}{\mathrm{d}t} = a^l - g_-(|p_2 - p_1|) + h_-(|q_2 - q_1|)\,\mathrm{sgn}(q_2 - q_1) - \gamma q_1 - (a^l + a^t - a), \tag{35}$$

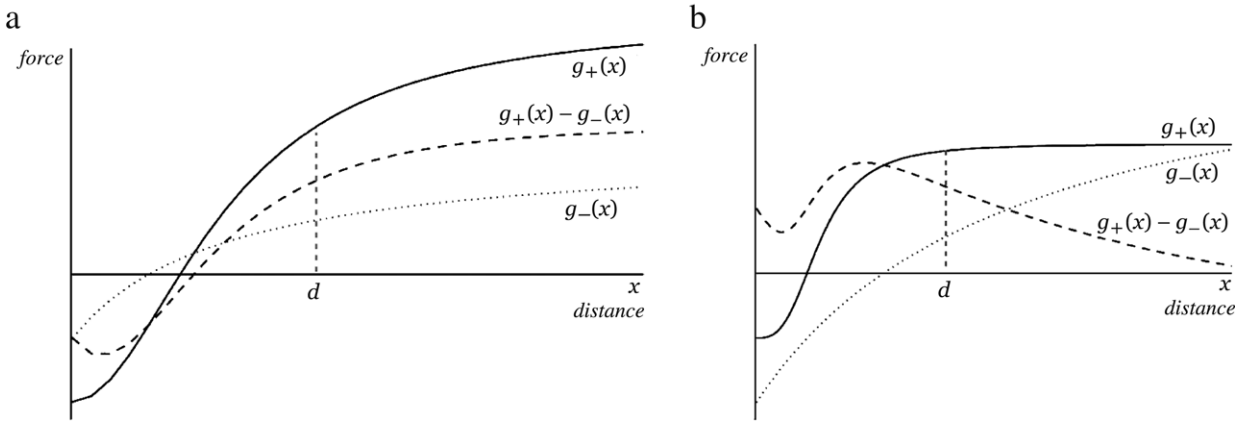

Fig. 5. (a) An example of interaction forces where the net force has positive slope at d. Here, $g_+(x) = 2[3x^2/(x^2+4^2) - 1]$, and $g_-(x) = 3x/(x+4) - 1$. (b) An example of interaction forces where the net force has negative slope at d. Here, $g_+(x) = (1/2)[3x^3/(x^3+2^3) - 1]$, and $g_-(x) = 3x/(x+8) - 1$.

$$\frac{\mathrm{d}q_i}{\mathrm{d}t} = a + g_+(|p_{i-1} - p_i|) - g_-(|p_{i+1} - p_i|) + h_+(|q_{i-1} - q_i|)\,\mathrm{sgn}(q_{i-1} - q_i) + h_-(|q_{i+1} - q_i|) \times \mathrm{sgn}(q_{i+1} - q_i) - \gamma q_i - (a^l + a^t - a), \tag{36}$$

$$\frac{\mathrm{d}q_n}{\mathrm{d}t} = a^t + g_+(|p_{n-1} - p_n|) + h_+(|q_{n-1} - q_n|) \times \mathrm{sgn}(q_{n-1} - q_n) - \gamma q_n - (a^l + a^t - a). \tag{37}$$

To investigate the linear stability of the school solution, we introduce a small perturbation to the equilibrium values of the velocity and the position of each particle in the moving frame:

$$p_i(t) = p_i^s + \delta_i(t), \tag{38}$$

$$q_i(t) = q_i^s + \omega_i(t), \tag{39}$$

where $\dot{p}_i^s = 0$, and $\dot{q}_i^s = 0$ for all i. Substituting Eqs. (38) and (39) into Eqs. (34)–(37), and expanding nonlinear terms in a Taylor series up to first order, we obtain

$$\frac{\mathrm{d}\delta_i}{\mathrm{d}t} = \omega_i, \tag{40}$$

$$\frac{\mathrm{d}\omega_1}{\mathrm{d}t} = -g_-(d) - g'_-(d)[\delta_1 - \delta_2] - h'_-(0)[\omega_1 - \omega_2] - \gamma\omega_1 + (a - a^t), \tag{41}$$

$$\frac{\mathrm{d}\omega_i}{\mathrm{d}t} = g_+(d) - g_-(d) + g'_+(d)[\delta_{i-1} - \delta_i] - g'_-(d)[\delta_i - \delta_{i+1}] \tag{42}$$

$$+ h'_+(0)[\omega_{i-1} - \omega_i] - h'_-(0)[\omega_i - \omega_{i+1}] - \gamma\omega_i + (2a - a^l - a^t), \tag{43}$$

$$\frac{\mathrm{d}\omega_n}{\mathrm{d}t} = g_+(d) + g'_+(d)[\delta_{n-1} - \delta_n] + h'_+(0)[\omega_{n-1} - \omega_n] - \gamma\omega_n + (a - a^l), \tag{44}$$

where $i = 1, \ldots, n$ in Eq. (40) and $i = 2, \ldots, n-1$ in Eq. (43) and where we have used $h_\pm(0) = 0$. Using Eqs. (28) and (29), we can reduce these equations to the following simplified form governing perturbations:

$$\frac{\mathrm{d}\delta_i}{\mathrm{d}t} = \omega_i, \tag{45}$$

$$\frac{\mathrm{d}\omega_1}{\mathrm{d}t} = -g'_-(d)[\delta_1 - \delta_2] - h'_-(0)[\omega_1 - \omega_2] - \gamma\omega_1, \tag{46}$$

$$\frac{\mathrm{d}\omega_i}{\mathrm{d}t} = g'_+(d)[\delta_{i-1} - \delta_i] - g'_-(d)[\delta_i - \delta_{i+1}] + h'_+(0)[\omega_{i-1} - \omega_i] - h'_-(0)[\omega_i - \omega_{i+1}] - \gamma\omega_i, \tag{47}$$

$$\frac{\mathrm{d}\omega_n}{\mathrm{d}t} = g'_+(d)[\delta_{n-1} - \delta_n] + h'_+(0)[\omega_{n-1} - \omega_n] - \gamma\omega_n, \tag{48}$$

where $i = 1, \ldots, n$ in (45) and $i = 2, \ldots, n-1$ in Eq. (47). The eigenvalues of the coefficient matrix associated with this linear system give stability information. It is not straightforward to obtain explicit expressions for the eigenvalues in the general case of Eqs. (45)–(48). However, when we simplify the system further for the case of following only one immediate neighbour in front, we

obtain the system

$$\frac{\mathrm{d}\delta_i}{\mathrm{d}t} = \omega_i, \tag{49}$$

$$\frac{\mathrm{d}\omega_1}{\mathrm{d}t} = -\gamma\omega_1, \tag{50}$$

$$\frac{\mathrm{d}\omega_i}{\mathrm{d}t} = g'_+(d)[\delta_{i-1} - \delta_i] + h'_+(0)[\omega_{i-1} - \omega_i] - \gamma\omega_i, \tag{51}$$

$$\frac{\mathrm{d}\omega_n}{\mathrm{d}t} = g'_+(d)[\delta_{n-1} - \delta_n] + h'_+(0)[\omega_{n-1} - \omega_n] - \gamma\omega_n. \tag{52}$$

When written in matrix form, the coefficient matrix corresponding to Eqs. (49)–(52) is a 2×2 block matrix with $n \times n$ blocks. To obtain the eigenvalues of this matrix we first simplify the determinant equation using the following result from [18]: given the block matrix

$$\begin{bmatrix} \mathbf{A} & \mathbf{B} \\ \mathbf{C} & \mathbf{D} \end{bmatrix},$$

where $\mathbf{A}$, $\mathbf{B}$, $\mathbf{C}$, and $\mathbf{D}$ are $m \times m$ matrices, if $\mathbf{A}$ and $\mathbf{B}$ commute, then

$$\det \begin{bmatrix} \mathbf{A} & \mathbf{B} \\ \mathbf{C} & \mathbf{D} \end{bmatrix} = \det [\mathbf{DA} - \mathbf{CB}] . \tag{53}$$

This result allows us to reduce the dimension of the matrix in the determinant formula for the eigenvalues. Assuming only forward (or, similarly, backward) sensing allows a further reduction to an upper (lower) triangular matrix, for which the determinant can be obtained from the product of the diagonal entries. The details of this calculation are given in Appendix A, where it is shown that the associated $2n$ eigenvalues are

$$\lambda_1 = 0, \tag{54}$$

$$\lambda_2 = -\gamma, \tag{55}$$

$$\lambda_\pm = -(h'_+(0) + \gamma)/2 \pm \sqrt{[(h'_+(0) + \gamma)/2]^2 - g'_+(d)}, \tag{56}$$

where the eigenvalues λ_+ and λ_- each have multiplicity $n - 1$. The zero eigenvalue in Eq. (54) characterizes the translational invariance of the solution, while λ_2 in Eq. (55) is always negative for $\gamma > 0$. However, in the absence of damping ($\gamma = 0$), the multiplicity of the zero eigenvalue is 2, indicating that the school solution is neutrally unstable. From Eq. (56), we obtain the stability conditions (guaranteeing $\lambda_\pm < 0$)

$$h'_+(0) + \gamma > 0, \tag{57}$$

$$g'_+(d) > 0. \tag{58}$$

Therefore, the contribution of the speed-dependent force is stabilizing if $h'_+(0) > 0$, and destabilizing if $h'_+(0) < 0$. However, even if the speed-dependence is destabilizing (i.e. if $h'_+(0) < 0$), the solution can still be stable if the damping, γ, is large enough to compensate in Eq. (57). This suggests that a nonzero damping term is indispensable for ensuring the stability of a perfect school solution. We have already shown that the conditions for existence of the perfect school are independent of velocity-dependent interaction forces; condition (57) also illustrates that $h_+(v)$ is not essential for the stability of the school solution. If $h_+(v) = 0$, i.e., there is no velocity-dependent force at all, then $\lambda_\pm = -\gamma/2 \pm \sqrt{(\gamma/2)^2 - g'_+(d)}$. Then, assuming Eq. (58) holds, the school solution remains stable if $\gamma > 0$.

On the other hand, the distance-dependent force is crucial, both for existence (as previously shown) and for stability of a perfect school solution. If $g_+(x) = 0$, $\lambda_\pm = 0, -(h'_+(0) + \gamma)$. Recalling that the multiplicity of λ_+ is $n - 1$, the school solution becomes neutrally unstable in the absence of the force $g_+(x)$, as the multiplicity of the zero eigenvalue is then n. Also note that the system can exhibit an oscillatory approach to steady state in the presence of complex conjugate eigenvalues; i.e., when $[(h'_+(0) + \gamma)/2]^2 < g'_+(d)$.

The results on school formation in 1D reveal that damping and the presence of a distance-dependent schooling force are key factors for the existence of a stable school pattern. Velocity-dependent schooling forces can make the school solution more or less stable depending on the sign of $h'_+(v)$, as shown in Eq. (57). We have shown that the school speed is determined by the autonomous self-propelling forces of particles at different locations within the school and is independent of the schooling forces. We also showed that school formation occurs even when each particle follows only its neighbour immediately ahead. This 'follower' school presents one minimal model of perfect school formation in 1D, and its simplicity has permitted an analytical description of the existence and stability of such schools.

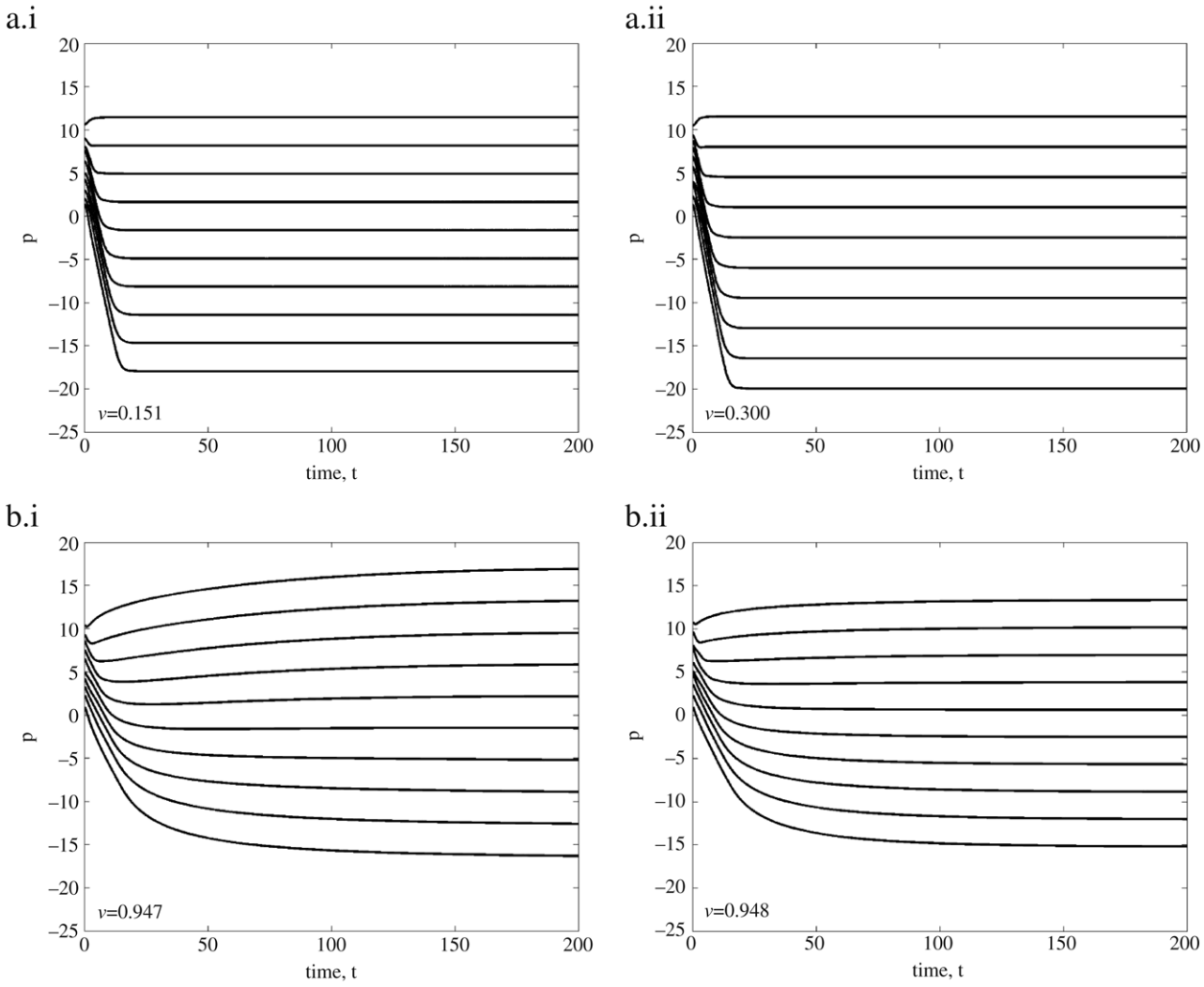

Fig. 6. 1D simulations showing position in a moving frame moving at velocity v as indicated. Interaction forces are as in (a) Fig. 5.a, and (b) Fig. 5.b. Self-propulsion terms are (a.i) $a^l = 0.5$, (a.ii) $a^l = 0.7$, (b.i) $a^l = 0.9$, (b.ii) $a^l = 0.8$, while $a = 0.1$ in all cases. In (a), higher school speed resulted in an increase in NND from 3.26 in (a.i) to 3.49 in (a.ii). The opposite occurred in (b), where higher school speed caused a decrease in d from 3.73 in (b.i) to 3.175 in (b.ii).

3.5. Numerical simulations in one dimension

We simulate the 1D model (10) and (11) in MATLAB using the solver ODE45, which integrates a system of ODEs with an embedded Runge–Kutta method. The algorithm is based on the Dormand–Prince 4(5) formulae, which uses a fourth- and fifth-order pair of methods. We show the case of distance-dependent interactions only; i.e., $h_\pm = 0$. Data is plotted in the moving frame, relative to the average velocity at $t = t_{\text{end}}$. Particles are initialized randomly in the interval [0,11]. The model inputs $g_\pm(x)$, a^l and a are chosen to satisfy Eq. (28), which in turn determines d. When d is known, a^t follows from Eq. (29), giving the self-propulsion that the last particle must produce to keep up with the school. The absolute magnitudes of the model inputs were chosen sufficiently small to avoid large changes in model variables at each time step. Relative magnitudes of model inputs were chosen so that motion was not dominated by any of the forces of autonomous propulsion, interaction, or drag.

We test two distinct examples of interaction forces to illustrate our results. In case 1 (Fig. 6(a)) we use forces as in Fig. 5(a), whereas in case 2 (Fig. 6(b)), the forces are as in Fig. 5(b). Increasing a^l in both cases generates a larger distance d, but, as noted in our analytic results, we expect velocity to increase in case 1 and decrease in case 2 as d is increased. These results are borne out by simulations.

Comparing the results presented here to those obtained in other models in which all-to-all interactions were considered [4,7,8,11], there are several important differences. First, the NND is determined by the self-propelling forces a^l, a and the interaction force function $g_+(x)$ (see Eqs. (28) and (29)). It is independent of the number of particles in the group. This is because only nearest-neighbour interactions are considered here. Increasing the number of particles does not increase the forces each particle experiences. Second, the "edge effect" that was typically observed in the other models is eliminated by making the edge particles behave differently based on their location in the group. Perfect schools cannot occur if the edge particles are not capable of sensing

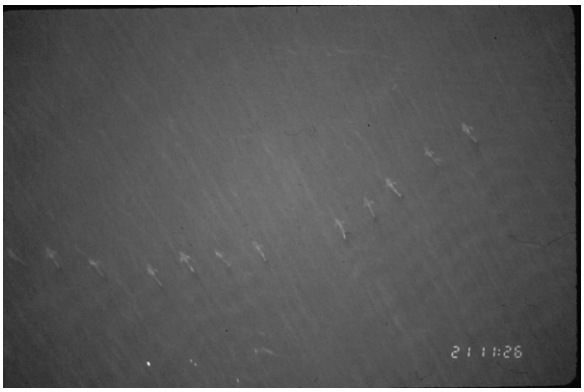

Fig. 7. An example of an approximate soldier formation in Atlantic bluefin tuna, courtesy of Dr. M. Lutcavage, Large Pelagics Research Center, UNH.

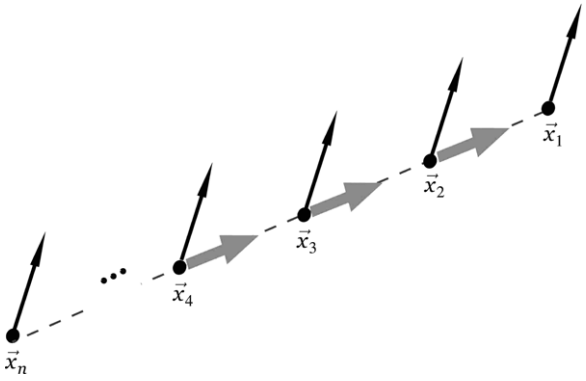

Fig. 8. A schematic diagram of individuals in soldier formation with frontal nearest-neighbour detection. Grey arrows indicate the direction of schooling force, while black arrows indicate the direction of motion.

their locations in the group and behaving accordingly. Third, the interaction functions that we use here are monotonic functions that typically violate the so-called H-stability conditions studied in [4,7]. H-stability is characterized by the conditions under which the NND approaches a finite nonzero value as the number of particles approaches infinity in an all-to-all coupled system. The conditions do not apply to the results presented here as only nearest-neighbour coupling is considered. Fourth, when a perfect school is slightly perturbed, the rate at which the system evolves toward the stable school pattern is governed by the real parts of the eigenvalues of the linearized system given by Eqs. (45)–(48). These eigenvalues are determined by the parameter γ and the slopes of the interactions forces $g'_{\pm}(d)$ and $h'_{\pm}(0)$. In the case when each particle follows only the immediate neighbour to its front, the eigenvalues are explicitly given by Eqs. (54)–(56). In the presence of complex valued eigenvalues, the approach to the stable school pattern can be oscillatory. The rate at which a perfect school solution is approached from an arbitrary initial condition is determined by both the linear and nonlinear effects of interaction forces.

4. The soldier formation in 2D space

Among the numerous types of schooling behaviour found in higher dimensions in nature is the *soldier formation*. Such schools are characterized by a roughly linear organization of individuals with a common heading in some (non-axial) direction. A school of this type formed by bluefin tuna is shown in Fig. 7. In the following treatment, we consider an idealization of soldier formations found in nature, such that all individuals have the same heading and velocity, and positions that lie on a straight line (see Fig. 8). The simple linear structure of such a school facilitates our analysis.

We apply the frontal nearest-neighbour interaction rule (i.e., $g_- = 0$) to a soldier formation of n particles, labeled so that 1 is the leader, and the remaining $n-1$ are followers. Under the chosen interaction regime, $\vec{x}_1$ is the nearest neighbour of $\vec{x}_2$, $\vec{x}_2$ is the nearest neighbour of $\vec{x}_3$ and so on. Note that the coupling of particles is not predetermined, but instead is determined by the group geometry. We neglect the velocity-dependent interactions (i.e., $h_\pm = 0$). The corresponding equations of motion for the system are

$$\frac{\mathrm{d}\vec{x}_1}{\mathrm{d}t} = \vec{v}_1, \tag{59}$$

$$\frac{\mathrm{d}\vec{v}_1}{\mathrm{d}t} = \vec{a}^l - \gamma\vec{v}_1, \tag{60}$$

and

$$\frac{\mathrm{d}\vec{x}_i}{\mathrm{d}t} = \vec{v}_i, \tag{61}$$

$$\frac{\mathrm{d}\vec{v}_i}{\mathrm{d}t} = \vec{a} - \gamma\vec{v}_i + \vec{f}_i, \tag{62}$$

for $i = 2, \ldots, n$. The schooling force $\vec{f}_i$ depends on the relative position of the ith individual with respect to its nearest neighbour, $(i-1)$, and thus has arguments

$$\vec{f}_i = \vec{f}_i(\vec{x}_{i-1} - \vec{x}_i).$$

Because we assume that individuals sense only what is in front of them, we have $\vec{f}_1 = \vec{0}$ for the leader.

4.1. Existence conditions for the soldier formation

In this section, Eqs. (59)–(62) are used to obtain the existence conditions for the soldier formation. In the soldier formation $\mathrm{d}\vec{v}_i/\mathrm{d}t = 0$, and so, we consider the formation as a 'moving-school' steady state for the system (henceforth referred to simply as steady state). We note that this steady state differs from a full steady state, wherein also $\mathrm{d}\vec{x}_i/\mathrm{d}t = 0$, i.e., where the aggregate is stationary, rather than moving.

The equation of motion (60) for the leader at steady state implies that

$$\vec{v} = \frac{\vec{a}^l}{\gamma}, \tag{63}$$

where $\vec{v}$ is the steady-state velocity of the leader. Note that because every individual moves at the same velocity in a steady-state school solution, $\vec{v}$ is also the velocity of all individuals in that school. Substituting this into the steady-state equation of motion for the ith individual gives the existence condition for a soldier formation:

$$\vec{f}_i^{\,s} = \vec{a}^l - \vec{a}, \quad i = 2, \ldots, n. \tag{64}$$

We express $\vec{f}_i^{\,s}$ as a unit direction vector (oriented along the axis of the school at steady-state) and a magnitude as in (5), giving $\vec{f}_i^{\,s} = g_+(d)\vec{u}$, where $\vec{u} = \vec{x}_{i-1,i}/|\vec{x}_{i-1,i}|$, and $d = |\vec{x}_{i-1,i}|$ is the distance between individuals at steady state.

We consider two cases: first, if $\vec{a}^l \neq \vec{a}$, then by (64), $g_+(d)\vec{u} = \vec{a}^l - \vec{a}$, i.e., the direction of axis of the school, $\vec{u}$, must be parallel to $\vec{a}^l - \vec{a}$. Similar to the case of a 1D school, the magnitude of $\vec{a}^l - \vec{a}$ determines the value(s) of $g_+(d)$ that guarantee the existence of such a school formation, i.e.,

$$g_+(d) = |\vec{a}^l - \vec{a}|. \tag{65}$$

For a monotonic function g_+, this uniquely determines the interindividual distance d along the axis of the school at steady state. This is an example of a stressed school in which interaction forces do not vanish at steady state. Once the parameters $\vec{a}^l$ and $\vec{a}$ are fixed and $g_+(x)$ is specified, $\vec{u}$, d, $\vec{v}$, and the bearing angle are all determined.

On the other hand, if $\vec{a}^l = \vec{a}$, then at steady state, $\vec{f}_i = \vec{a}^l - \vec{a} = \vec{0}$, i.e., the school is stress-free and there is no restriction on the bearing angle of the axis of the school.

4.2. Stability analysis

In the soldier formation, the cohesiveness of the group can be examined in terms of the stability of the system to small perturbations about the steady state; i.e., the local stability. The stability analysis of the soldier formation in 2D follows closely the analysis of 1D schools.

The geometry of a soldier formation allows some simplification in analysis by a judicious choice of orientation of axes. Specifically, we align our coordinate system so that the x-axis lies along the line of individuals. Then the y-components of the particle positions are zero at the steady-state soldier formation solution. Note, however, that unlike 1D motion, the individuals here move (in general) in some direction other than the x-axis. Thus we write

$$\vec{x}_1^{\,s} = (0\,,\,0), \qquad \vec{x}_2^{\,s} = (d\,,\,0),\ \ldots,\ \vec{x}_i^{\,s} = ((i-1)d\,,\,0)\ ,\ldots,\ \vec{x}_n^{\,s} = ((n-1)d\,,\,0).$$

Henceforth, we display only calculations for the ith equation, but this implicitly represents all $i = 1, \ldots, n$. We transform to a frame of reference moving with the school velocity at steady state (Eq. (63)). We let

$$\vec{x}_i = \vec{p}_i + \vec{v}t,$$
$$\vec{v}_i = \vec{q}_i + \vec{v}.$$

We substitute these expressions into (59)–(62) to obtain

$$\frac{\mathrm{d}(\vec{p}_1 + \vec{v}t)}{\mathrm{d}t} = \vec{q}_1 + \vec{v}, \tag{66}$$

$$\frac{\mathrm{d}(\vec{q}_1 + \vec{v})}{\mathrm{d}t} = \vec{a}^l - \gamma\,(\vec{q}_1 + \vec{v})\,, \tag{67}$$

$$\frac{\mathrm{d}(\vec{p}_i + \vec{v}t)}{\mathrm{d}t} = \vec{q}_i + \vec{v}, \quad i = 2, \ldots, n \tag{68}$$

$$\frac{\mathrm{d}(\vec{q}_i + \vec{v})}{\mathrm{d}t} = \vec{a} - \gamma\,(\vec{q}_i + \vec{v}) + \vec{f}_i, \quad i = 2, \ldots, n. \tag{69}$$

Simplifying these equations, noting that $\gamma\vec{v} = \vec{a}^l$, we obtain the moving-frame equations of motion:

$$\frac{\mathrm{d}\vec{p}_1}{\mathrm{d}t} = \vec{q}_1, \tag{70}$$

$$\frac{\mathrm{d}\vec{q}_1}{\mathrm{d}t} = -\gamma\vec{q}_1, \tag{71}$$

$$\frac{\mathrm{d}\vec{p}_i}{\mathrm{d}t} = \vec{q}_i, \quad i = 2, \ldots, n, \tag{72}$$

$$\frac{\mathrm{d}\vec{q}_i}{\mathrm{d}t} = \vec{a} - \vec{a}^l + \vec{f}_i - \gamma\vec{q}_i, \quad i = 2, \ldots, n. \tag{73}$$

The arguments of $\vec{f}_i$ are now $\vec{f}_i = \vec{f}_i(\vec{p}_{i-1} - \vec{p}_i)$, though we continue to omit these arguments unless needed for clarity. To summarize, $\vec{p}_i$ represents the position of individual i in the moving frame, and $\vec{q}_i$ represents the velocity of individual i in the moving frame. The soldier formation is a steady-state solution to this system, and thus at steady state, $\vec{q}_i = 0$ and $\vec{a} - \vec{a}^l + \vec{f}_i = 0$, which gives the existence condition in (64), and $\vec{p}_i^s = \hat{\mathbf{e}}_1(i-1)d$, where $\hat{\mathbf{e}}_1$ is the unit vector $(1\,,\,0)$. Next, we perform a stability analysis on our moving-coordinate 2D variables $\vec{p}_i$ and $\vec{q}_i$. We introduce small perturbations in position $\vec{\delta}_i$ and velocity $\vec{\omega}_i$ about the steady state; i.e.,

$$\vec{p}_i(t) = \vec{p}_i^s + \vec{\delta}_i(t) = \hat{\mathbf{e}}_1(i-1)d + \vec{\delta}_i(t),$$

and

$$\vec{q}_i(t) = \vec{q}_i^s + \vec{\omega}_i(t) = \vec{\omega}_i(t),$$

where $\hat{\mathbf{e}}_1$ is a unit vector in the x-direction. Substituting these perturbations into Eqs. (70)–(73) and noting that time derivatives of steady-state variables are 0, we get

$$\frac{\mathrm{d}\vec{\delta}_1}{\mathrm{d}t} = \vec{\omega}_1, \tag{74}$$

$$\frac{\mathrm{d}\vec{\omega}_1}{\mathrm{d}t} = -\gamma\omega_1, \tag{75}$$

$$\frac{\mathrm{d}\vec{\delta}_i}{\mathrm{d}t} = \vec{\omega}_i, \quad i = 2, \ldots, n, \tag{76}$$

$$\frac{\mathrm{d}\vec{\omega}_i}{\mathrm{d}t} = (\vec{a} - \vec{a}^l) + \vec{f}_i - \gamma\omega_i, \quad i = 2, \ldots, n. \tag{77}$$

We proceed by expanding the nonlinear term, $\vec{f}_i$ in a Taylor series. We first rewrite $\vec{f}_i$ as

$$(f_{ix}, f_{iy}) = \vec{f}_i(\vec{z}_i) = g_+(|\vec{z}_i|)\frac{\vec{z}_i}{|\vec{z}_i|} = g_+(|\vec{z}_i|)\left(\frac{z_{ix}}{|z_i|}, \frac{z_{iy}}{|z_i|}\right),$$

where

$$\langle z_{ix}, z_{iy}\rangle \equiv \vec{z}_i = \vec{p}_{i-1} - \vec{p}_i = -\hat{\mathbf{e}}_1 d + \vec{\delta}_{i-1} - \vec{\delta}_i, \tag{78}$$

and

$$|\vec{z}_i| = \sqrt{z_{ix}^2 + z_{iy}^2}.$$

That is, $\vec{f}_i$ is oriented in the direction of the vector connecting two neighbouring individuals, with a magnitude dependent on the distance between the two individuals. The Taylor expansion of $\vec{f}_i$ is

$$\vec{f}_i = \vec{f}_i(-\hat{\mathbf{e}}_1 d) + \left(\frac{\partial \vec{f}_i}{\partial \vec{z}_i}|_{\vec{z}_i=\vec{z}_i^s}\right) \cdot \left[\vec{z}_i - \vec{z}_i^s\right] + \cdots, \tag{79}$$

where the expression in braces is a Jacobian matrix, i.e., the partial derivatives of f_{ix} and f_{iy} with respect to z_{ix} and z_{iy} coordinates. The Jacobian matrix in Eq. (79) evaluated at steady state is given by

$$Df \equiv \left(\frac{\partial \vec{f}_i}{\partial \vec{z}_i}|_{\vec{z}_i=\vec{z}_i^s}\right) = \begin{bmatrix} g'_+(d) & 0 \\ 0 & g_+(d)/d \end{bmatrix}.$$

Details of this calculation are contained in Appendix B. Df is independent of the equation index i, and is thus identical for all individuals $i = 2, \ldots, n$. Substituting Df into the Taylor expansion of $\vec{f}_i$ in Eq. (79) and noting from Eq. (78), and Eq. (99) in Appendix B that

$$\vec{z}_i - \vec{z}_i^s = \vec{\delta}_{i-1} - \vec{\delta}_i, \tag{80}$$

we now have

$$\vec{f}_i = \vec{f}_i(-\hat{\mathbf{e}}_1 d) + Df \cdot [\vec{\delta}_{i-1} - \vec{\delta}_i] + \cdots. \tag{81}$$

Furthermore, because at steady state we have $\vec{f}_i(-\hat{\mathbf{e}}_1 d) = \vec{a}^l - \vec{a}$, it follows that for the small perturbation,

$$\vec{f}_i \simeq \vec{a}^l - \vec{a} + Df \cdot [\vec{\delta}_{i-1} - \vec{\delta}_i].$$

We now use this linear approximation for $\vec{f}_i$ in Eq. (77), resulting in

$$\frac{\mathrm{d}\vec{\omega}_i}{\mathrm{d}t} = \vec{a} - \vec{a}^l + (\vec{a}^l - \vec{a} + Df \cdot [\vec{\delta}_{i-1} - \vec{\delta}_i]) - \gamma \vec{\omega}_i.$$

Canceling out the terms and combining with Eqs. (74)–(76) gives the following system:

$$\frac{\mathrm{d}\vec{\delta}_1}{\mathrm{d}t} = \vec{\omega}_1, \tag{82}$$

$$\frac{\mathrm{d}\vec{\omega}_1}{\mathrm{d}t} = -\gamma \omega_1, \tag{83}$$

$$\frac{\mathrm{d}\vec{\delta}_i}{\mathrm{d}t} = \vec{\omega}_i, \quad i = 2, \ldots, n \tag{84}$$

$$\frac{\mathrm{d}\vec{\omega}_i}{\mathrm{d}t} = Df \cdot [\vec{\delta}_{i-1} - \vec{\delta}_i] - \gamma \vec{\omega}_i, \quad i = 2, \ldots, n. \tag{85}$$

The matrix expression of this system is a 2×2 block matrix with $2n \times 2n$ blocks. The eigenvalue equation is formulated in determinant form, and the commutativity of the blocks of the associated matrix allows for a simplification of the determinant using Eq. (53). The eigenvalue calculation is thus reduced to calculating the determinant of an $n \times n$ block-triangular matrix with 2×2 blocks, which is given by the product of the determinants of the diagonal blocks. The matrix form of Eqs. (82)–(85) and the eigenvalue calculations are given in Appendix B. The coefficient matrix associated with Eqs. (82)–(85) has eigenvalues

$$\lambda = 0, \quad \text{with multiplicity 2,} \tag{86}$$

$$\lambda = -\gamma, \quad \text{with multiplicity 2,} \tag{87}$$

$$\lambda = -\frac{\gamma}{2} \pm \frac{\sqrt{\gamma^2 - 4g'_+(d)}}{2}, \qquad \text{each with multiplicity } n-1 \tag{88}$$

$$\lambda = -\frac{\gamma}{2} \pm \frac{\sqrt{\gamma^2 - 4g_+(d)/d}}{2}, \qquad \text{each with multiplicity } n-1. \tag{89}$$

The first eigenvalues, $\lambda = 0$ with multiplicity 2, indicates a translational invariance in 2D space. The next distinct eigenvalue, $\lambda = -\gamma$ is always negative when damping is present, $\gamma > 0$. This further indicates the importance of a drag term for the stability of solutions.

The remaining eigenvalues have negative real parts provided both

$$g'_+(d) > 0, \tag{90}$$

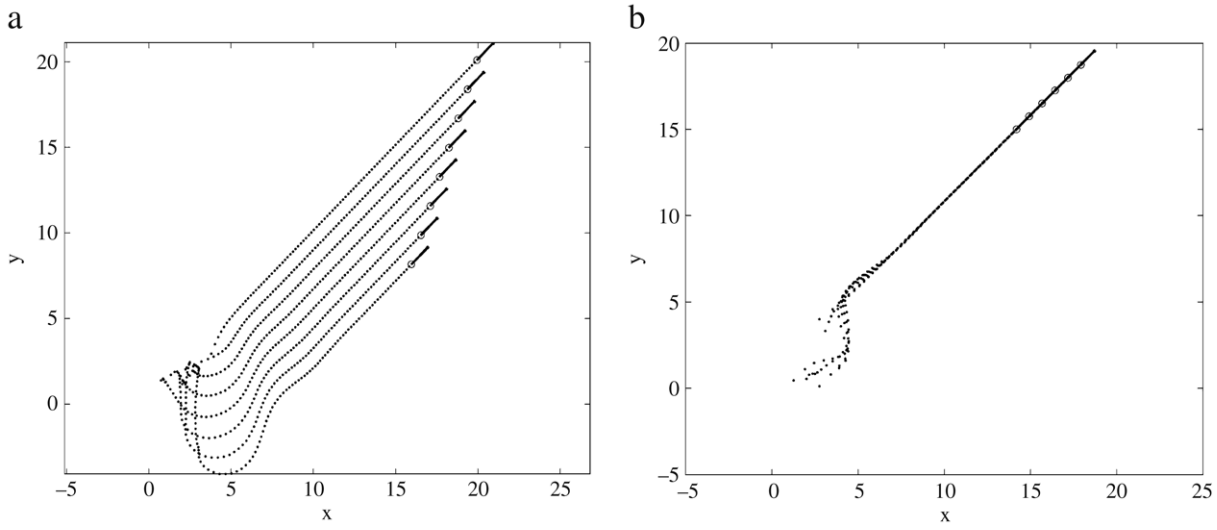

Fig. 9. Numerical simulations in 2D for (a) 8 particles with $\vec{a}^l = [0.1, 0.1]$, $\vec{a} = [0, -0.2]$ and (b) 6 particles with $\vec{a}^l = [0.1, 0.1]$, $\vec{a} = [0, 0]$. Trajectories are plotted through time. Note in (a) that the solution line connecting individuals is oriented in the direction of $\vec{a}^l - \vec{a} = [0.1, 0.3]$, while the school velocity at steady state is $\vec{v} = [0.2, 0.2]$. In (b), both the solution line and school velocity are in the same direction, with $\vec{a}^l = [0.1, 0.1]$, $\vec{v} = [0.2, 0.2]$.

$$g_+(d) > 0. \tag{91}$$

Interpreted in terms of stability of the school solution, Eqs. (90) and (91) imply that the schooling force acting to maintain the school must be attractive at the NND d. Additionally, this attractive force should increase if individuals with spacing d try to move further apart.

4.3. Numerical simulation of the soldier formation

We perform simulations in two dimensions using single-neighbour interactions, with neighbour detection only in the frontal plane ($g_- = 0$). We include no velocity-dependent interactions ($h_\pm = 0$). We choose an exponential interaction function following Eq. (33), as $g_+(x) = 0.5(\exp(-x/50) - 2\exp(-x/1))$. Eqs. (59)–(62) are evolved using ODE45 as in the 1D simulations. Initial positions are assigned randomly in $[0, 4] \times [0, 4]$, and we set $\gamma = 0.5$.

We first test two distinct cases of $\vec{a}^l$ and $\vec{a}$ values. In case 1 (Fig. 9(a)) $\vec{a}^l \neq \vec{a} \neq \vec{0}$, while in case 2 (Fig. 9(b)), $\vec{a}^l \neq \vec{a} = \vec{0}$. As noted in our analytical results, we expect the soldier formation to move in the direction of $\vec{a}^l$, while the solution line connecting individuals is oriented in the direction of $\vec{a}^l - \vec{a}$. In case 1, this corresponds to a school directed non-axially to the solution line, while in case 2, the solution line and school direction coincide, leading to a trail-following group. The NND in these solutions is determined by Eq. (65). For the cases in Fig. 9(a) and 9(b), $d = 1.7949$ and 1.055 respectively. The difference in d between the two cases is due to the difference in the value of $|\vec{a}^l - \vec{a}|$ but not the difference in the number of particles. Because only nearest-neighbour interactions are considered here, this distance remains unchanged as the number of particles is increased. These analytical results are confirmed by simulations shown in Fig. 9. Although our stability results are only local, the simulations suggest that the soldier formation is a globally stable pattern for the specific choice of parameter values in Fig. 9(a). In a follow-up study [10], we found that the milling formation could coexist with the soldier formation when the force function $g_+(x)$ is biphasic. In that case, different initial conditions determine which pattern will eventually emerge. Unlike the soldier formation, the existence of a milling solution and the NND both depend on the number of particles for a fixed choice of the force function.

In Section 4.1, we mentioned the case when $a^l = a$, which implies no restriction on the bearing angle of individuals. Eq. (65) implies that the zero of $g_+(x)$ gives the individual distance d at steady state for such groups. Fig. 10 shows examples of such configurations. Note that individual distance at steady state remains constant at $d = 0.7$, though the relative angles between neighbours is determined by initial conditions.

In previous simulations, we used the interaction functions that allowed stable schools to arise. However, if we choose $g_+(x)$ so that $g'_+(x)$ is negative for all $x > 0$, then we fail to satisfy the stability condition in Eq. (90). We explore the motion of particles under such conditions in simulations (Fig. 11). In these simulations, particles tend to organize in moving pairs which remain together due to close-range attraction. The path traced out by these pairs appears to be very sensitive to initial conditions, and does not follow a predictable pattern. Further simulations with such 'stability-breaking' interaction forces reveal the presence of numerically stable mill solutions in which particles rotate around an invariant circle. These solutions require a closed curve of interaction connections between particles in order to evolve. The existence and stability of such mill solutions form the topic of a forthcoming paper [10].

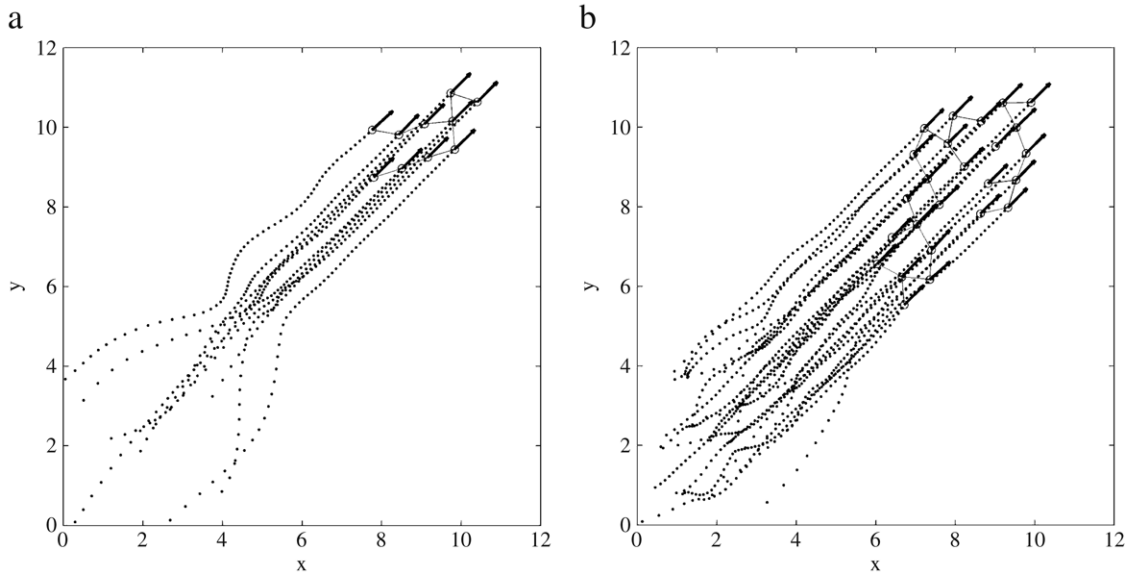

Fig. 10. Numerical simulations in 2D, for (a) 10 particles and (b) 25 particles with $\vec{a}^l = \vec{a} = [0.1, 0.1]$, and $g_+(x) = 0.5(\exp(-x/50) - 2\exp(-x/1))$. Trajectories are plotted through time, and grey arrows indicate the interactions between nearest neighbours. Note that individuals have constant spacing between nearest neighbours, but are not restricted to a particular relative angle with nearest neighbours.

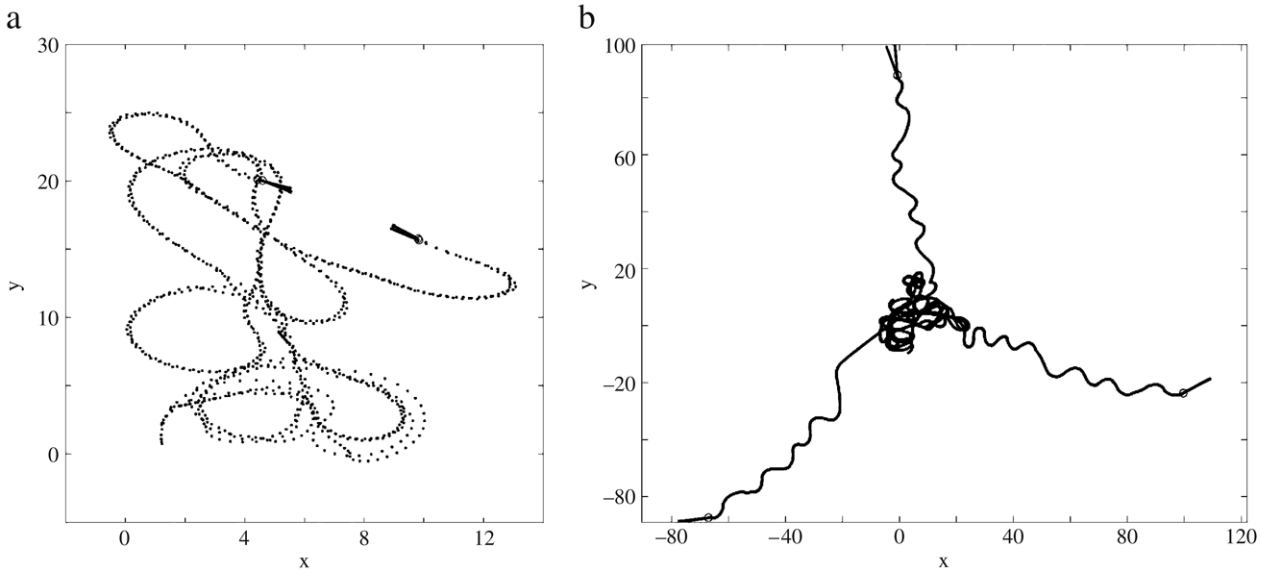

Fig. 11. Numerical simulations in 2D with $g_+(x) = 1 - x/2$, which corresponds to (rather non-physical) short-range attraction and long-range repulsion. Trajectories are plotted in time for (a) 4 particles evolved to $t = 40$, and (b) 6 particles evolved to $t = 300$. Individuals group in pairs (though due to overlapping, some pairs appear as a single particle), and these pairs follow unpredictable trajectories.

5. Schools in the form of 2D arrays

We have thus far been primarily concerned with 1D and quasi-1D formations of particles. However, extending these ideas to schools in the form of regular 2D arrays (i.e., a perfect school in 2D) is both a logical step in the mathematical analysis, and is more relevant to many observed biological aggregates. This extension to 2D brings a number of challenges to our analytical approach. First of all, similar to the case of 1D schools in which the tail particle should be aware of its special position in the group and behave differently to maintain the school, particles located at the edges of a 2D array should also behave differently than particles in the interior. Confounding the issue further, the number of edge particles change as the specific shape of the array changes. Thus, it is very difficult to study 2D arrays in a general form since there exist many possible 2D shapes for a group composed of a large number

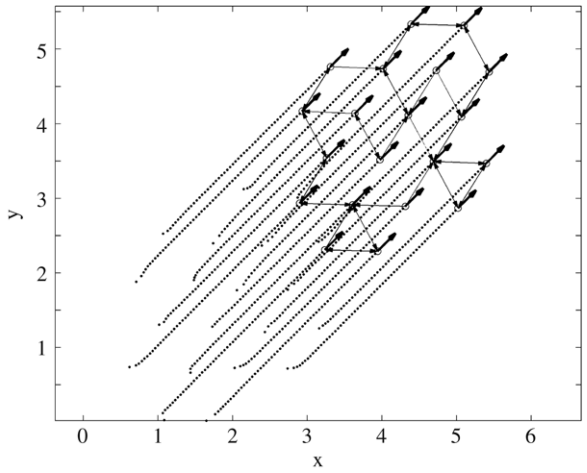

Fig. 12. Numerical simulation of two nearest-neighbour interactions. Trajectories are plotted through time. Note that the particles, initially perturbed, evolve to a regular tiling of the plane with individual distance $d = 0.707$.

of particles. For groups of small numbers of particles, some analytical insights can be made, though these are shape dependent and not generalizable.

However, numerical simulations can provide insight into the mechanisms of forming schools of 2D arrays that tile the plane in a regular fashion. If we restrict our discussion to the models in which each particle only follows one closest neighbour, we must apply the restriction $\vec{a}^l = \vec{a}$, as otherwise a soldier formation would emerge (assuming the corresponding stability conditions are satisfied).

For a group of particles that follow only one nearest neighbour in its frontal visual field with $\vec{a}^l = \vec{a} \neq \vec{0}$, many stress-free patterns can occur depending on the initial conditions. The NND remains fixed in all these patterns since it is determined by the value of d that makes $g_+(d) = 0$ (note that $g_+(x)$ has only a single zero in our simulations). Two examples are shown in Fig. 10. For the $g_+(x)$ function chosen in these simulations, $d = 0.707$ in both panels. Since interactions only occur between nearest neighbours, this distance does not change as the number of particles increases. The bearing angle between neighbours is sensitive to initial conditions, such that small changes in initial conditions can lead to large changes in the shape of the group that evolves. To generate a perfect school in 2D we could initialize particles in a regular array, and this array would persist in time so long as it is not subject to noise. However, in both irregular and regular arrays, perturbations can alter the configuration after such groups have been formed. This is due to the fact that the magnitude of the interacting force is only distance dependent, and thus there exists a circular arc of positions around a preceding particle which its follower can occupy while remaining equidistant from its neighbour. Then upon undergoing a perturbation, a particle is free to return to any point on this arc, and not necessarily to its original point in the undisturbed array. We also note that velocity-dependent forces act to align the group, but do not contribute to maintaining a fixed bearing angle.

Then the question arises as to what minimal mechanisms can generate a stable 2D perfect school solution. We have found that by increasing both the number of neighbours sensed by each particle and the sensing region, we can generate schools that are stable in numerical simulations.

Consider a group of particles, each interacting with two nearest neighbours. We no longer restrict interactions to the front of a particle, and instead assume that individuals can sense neighbours in any direction. By removing the restriction of sensing in the frontal region, we eliminate the edge issues discussed earlier. We use a single force for all directions of interaction, given by $g(x) = 0.5(\exp(-x/50) - 2\exp(-x/1))$, as in earlier examples. Particles are initialized in a hexagonal tiling, where each hexagon contains an individual in the middle, such that the entire school can be broken into groups of particles forming equilateral triangles. This tiling is then perturbed, and this perturbed tiling is taken as the initial condition. Such a system was found in numerical simulations to evolve to a regular tiling of fixed interindividual distance d that moves as a rigid body (see Fig. 12). Stability analysis for such a solution is quite difficult using analytical techniques introduced here for two reasons: it is difficult to label individuals to generate structure in stability matrices, and due to the geometry, individuals can change which particle they interact with as a result of a small perturbation. This latter fact actually serves to stabilize the solution by maintaining proper distance between individuals even when a direct interaction may not exist, as a perturbation closer to a neighbour would cause interaction with this neighbour and consequent return to the initial relative position.

Simulations of 2D schools that yield a large variety of different school patterns with different shapes and features have been carried out in the presence of small noise, using various interaction schemes. Some groups form perfect schools, while some exhibit variation at the boundary of the school, both spatially and temporally. A detailed exploration of all of these numerically observed patterns lies outside the focus of this paper.

6. Discussion

The formation of cohesive schools is a phenomenon that occurs in a number of aggregating organisms. Among the most striking and common examples are flocks of birds and schools of fish. These groups provide motivation for a host of mathematical models which seek to lend insight into the behavioural algorithms used to generate school patterns. In contrast to the Eulerian modeling approach (see, e.g., [21–23]) which gives mean field properties and is useful in modeling the global dynamics of large populations, we use a Lagrangian approach. By modeling the individual particles, we gain information on spacing and heading that is lost in the Eulerian approach at the expense of greatly increasing the dimension of the associated system of ODEs. However, in the case of some particular solutions, these large systems of nonlinear ODEs permit analytical insights. In our study, we are concerned with relatively basic interactions between particles, and geometrically simple solutions that such interactions permit.

Our modeling approach takes as inputs the inherent behaviour of individuals, as well as a functional description of how they interact with one another. With these inputs, the model can then address [a], whether or not the school can exist, [b], if it can exist, the spacing and school velocity that prevails at steady state, [c], the geometry of the school; that is, how individuals align with other individuals, and how they move in relation to this alignment, and [d], whether or not a school solution is linearly stable under small perturbations. The simplicity of our approach allows us to directly connect the features of existence, stability and school geometry to basic features of interaction functions and model parameters. Our results do not qualitatively depend on the specific choice of the schooling functions $g_{\pm}(x)$ and $h_{\pm}(x)$, provided these functions satisfy the criteria established in this paper.

In 1D, we studied schools formed by interactions to the front, and then, interactions both to the front and back. We obtained the existence conditions for such schools to exist, and analytically obtained school velocity and individual distance d that prevail at the perfect school solution. We were able to relate how the slope of the "net schooling force function" $g_+ - g_-$ near d determines the relationship between velocity and spacing in a school, and this relationship was shown in simulations. We then obtained the stability conditions in the case of interactions to the front, with the result that both $h'_+(0) + \gamma$ and $g'_+(d)$ be positive to guarantee stability.

Using essentially the same analytical techniques as in 1D, we explored the soldier formations of particles organized in a line, moving in some direction non-axial to the line. We obtained the existence conditions which provided analytical descriptions of spacing, heading direction, school speed and the direction of the line of individuals. We performed a stability analysis on such schools, with the result that both $g_+(d)$ and $g'_+(d)$ must be positive to guarantee stability. Following our analysis, we performed numerical simulations of the model in 2D, showing that the soldier formation appears to be globally stable with respect to random initial conditions when both the existence conditions and local stability conditions are satisfied, and $\vec{a}^l \neq \vec{a}$. In the case of $\vec{a}^l = \vec{a}$, we find no restriction on relative angle between neighbours, and individuals arrange themselves with constant distance, but with relative angles dependent on initial conditions. We then explored the situations in which the local stability conditions were not met, which leads to individuals pairing off and each pair following an unpredictable trajectory. Lastly, we presented a minimal mechanism to generate perfect schools in 2D such that particles form a regular array that moves at a constant speed. This solution was shown to be stable in numerical simulations using a typical interaction function.

We have shown analytically that following one neighbour is sufficient to generate stable perfect schools in 1D, while following two neighbours were shown numerically to generate stable perfect schools in 2D. This leads to a conjecture that interactions with three neighbours should suffice to generate stable perfect schools in 3D. Exploring such questions analytically and computationally forms the basis of our ongoing work.

Although in this paper, we have studied only the simple arrangements of particles, our approach clearly demonstrates how the properties of each aspect of the model influences the observed features of the school. Although we have emphasized simplicity in formulating minimal mechanisms for school formation, our results are nevertheless general, in that we have avoided assuming particular functional forms to obtain the results. Also, the simplicity of our approach underscores the considerable variation in the class of solutions, and the sensitivity of these solutions to how the particles interact.

The study of the formation of social aggregates in self-propelled particles has become increasingly active. A number of recent studies have revealed a large number of interesting patterns in groups of particles coupled through pairwise interactions [4,7,8,11]. In these studies, all-to-all interactions are considered and the limiting behaviour of the group as the number of particles approaches infinity has been shown to be crucial in determining some important features of the aggregate patterns that can occur. The patterns that emerge in these systems are often not regular and may even be meta-stable or transient states [7]. Results presented in this work represent a rare distinct attempt at focusing on minimal mechanisms that are sufficient for generating regular school patterns that are dynamically stable. We showed that nearest-neighbour interactions are sufficient for generating regular school patterns with some crucial characteristic features that are independent of the number of particles in the group. A detailed analysis of the similarity and difference between the aggregate patterns in all-to-all coupled and nearest-neighbour coupled self-propelling particles could lead to experimental criteria that allow us to check which one is closer to reality.

Acknowledgements

This work was funded by NSERC discovery grants to Y.X. Li and L. Edelstein-Keshet. R. Lukeman was funded by an NSERC graduate scholarship, and by a UBC University Graduate Fellowship.

Appendix A. The stability analysis in 1D

We write (45)–(48) in matrix form as

$$\frac{\mathrm{d}}{\mathrm{d}t}\begin{bmatrix}\delta_1\\ \delta_2\\ \vdots\\ \delta_n\\ \omega_1\\ \omega_2\\ \vdots\\ \omega_n\end{bmatrix} = \left[\begin{array}{ccc|ccc} & 0 & & & I & \\ -- & -- & -- & -- & -- & -- \\ & V & & & U & \end{array}\right]\begin{bmatrix}\delta_1\\ \delta_2\\ \vdots\\ \delta_n\\ \omega_1\\ \omega_2\\ \vdots\\ \omega_n\end{bmatrix}, \tag{92}$$

where all the submatrices are $n \times n$. In particular, 0 is the zero matrix and I is the identity matrix. V and U are given by

$$V = \begin{bmatrix} -g'_-(d) & g'_-(d) & 0 & 0 & \cdots & 0 & 0 \\ g'_+(d) & -\sigma & g'_-(d) & 0 & \cdots & 0 & 0 \\ 0 & g'_+(d) & -\sigma & g'_-(d) & \cdots & 0 & 0 \\ \cdots & \cdots & \cdots & \cdots & \cdots & \cdots & \cdots \\ 0 & 0 & 0 & 0 & \cdots & -\sigma & g'_-(d) \\ 0 & 0 & 0 & 0 & \cdots & g'_+(d) & -g'_+(d) \end{bmatrix},$$

$$U = \begin{bmatrix} -h'_-(0)-\gamma & h'_-(0) & 0 & 0 & \cdots & 0 & 0 \\ h'_+(0) & -s & h'_-(0) & 0 & \cdots & 0 & 0 \\ 0 & h'_+(0) & -s & h'_-(0) & \cdots & 0 & 0 \\ \cdots & \cdots & \cdots & \cdots & \cdots & \cdots & \cdots \\ 0 & 0 & 0 & 0 & \cdots & -s & h'_-(0) \\ 0 & 0 & 0 & 0 & \cdots & h'_+(0) & -h'_+(0)-\gamma \end{bmatrix},$$

where $s = h'_+(0) + h'_-(0) + \gamma$ and $\sigma = g'_+(d) + g'_-(d)$. Note that U and V are tridiagonal matrices.

The eigenvalues of J are obtained by solving

$$\Lambda(\lambda) \equiv \det[\lambda I - J] = \det\begin{bmatrix}\lambda I & -I \\ -V & \lambda I - U\end{bmatrix} = 0. \tag{93}$$

We can simplify this eigenvalue equation via the result stated in Eq. (53). In this case, because λI and $-I$ commute, then

$$\det[\lambda I - J] = \det[\lambda^2 I - U\lambda I - IV] = \det[\lambda^2 I - \lambda U - V]. \tag{94}$$

Since U and V are tridiagonal matrices, so is the matrix in (94). We can now write (93) explicitly as

$$\det\begin{bmatrix} \chi+\eta & \alpha & 0 & \cdots & 0 & 0 \\ \eta & \chi & \alpha & \cdots & 0 & 0 \\ \cdots & \cdots & \cdots & \cdots & \cdots & \cdots \\ 0 & 0 & 0 & \cdots & \chi & \alpha \\ 0 & 0 & 0 & \cdots & \eta & \chi+\alpha \end{bmatrix} = 0, \tag{95}$$

where $\chi = \lambda^2 + s\lambda + \sigma$, $\eta = -h'_+(0)\lambda - g'_+(d)$, and $\alpha = -h'_-(0)\lambda - g'_-(d)$.

Thus, the eigenvalue equation is a polynomial of λ that is defined by the determinant of a tridiagonal matrix. Although the determinant can be calculated recursively, the complexity of the resulting formula prevents us from solving the eigenvalues easily. However, the eigenvalues are easily solvable in the case when either g_+ or g_- is absent, i.e., when individuals interact only with neighbours in front or behind them.

Let us consider the case that particles see only what is in front of them. This is the model for schools formed by following one immediate predecessor. In this case, $h'_-(0) = g_-(d) = 0$. Thus, $\alpha = 0$, $\chi = \lambda^2 + (h'_+(0) + \gamma)\lambda + g'_+(d)$, and $\chi + \eta = \lambda^2 + \gamma\lambda = \lambda(\lambda + \gamma)$. The eigenvalue equation now requires only the determinant of a triangular matrix which is given by the simple formula $\Lambda(\lambda) = (\chi + \eta)\chi^{n-1}$. Thus, the eigenvalues are determined by

$$\Lambda(\lambda) = (\chi + \eta)\chi^{n-1} = \lambda(\lambda + \gamma)[\lambda^2 + (h'_+(0) + \gamma)\lambda + g'_+(d)]^{n-1} = 0. \tag{96}$$

Therefore, the eigenvalues are $\lambda_1 = 0$, $\lambda_2 = -\gamma$, and $\lambda_\pm = -(h'_+(0) + \gamma)/2 \pm \sqrt{[(h'_+(0) + \gamma)/2]^2 - g'_+(d)}$. Both λ_+ and λ_- have multiplicity $n - 1$.

Similarly, if each particle can only detect the a particle behind but not a particle in front (a rather peculiar situation), $\eta = 0$ and $\chi = \lambda^2 + (h'_-(0) + \gamma)\lambda + g'_-(d)$. Therefore,

$$\Lambda(\lambda) = (\chi + \alpha)\chi^{n-1} = \lambda(\lambda + \gamma)[\lambda^2 + (h'_-(0) + \gamma)\lambda + g'_-(d)]^{n-1} = 0. \tag{97}$$

The eigenvalues are $\lambda_1 = 0$, $\lambda_2 = -\gamma$, and $\lambda_\pm = -(h'_-(0) + \gamma)/2 \pm \sqrt{[(h'_-(0) + \gamma)/2]^2 - g'_-(d)}$. Both λ_+ and λ_- have $n - 1$ multiplicity. We find that the roles of $h'_-(0)$ and $g'_-(d)$ in determining the stability are quite similar to the roles of $h'_+(0)$ and $g'_+(d)$ in the case of forward sensing.

Appendix B. Stability analysis for the soldier formation in 2D space

We can explicitly write the Jacobian matrix $\frac{\partial \vec{f}_i}{\partial \vec{z}_i}$ in Eq. (79) as

$$J = \begin{bmatrix} \frac{\partial f_{ix}}{\partial z_{ix}} & \frac{\partial f_{ix}}{\partial z_{iy}} \\ \frac{\partial f_{iy}}{\partial z_{ix}} & \frac{\partial f_{iy}}{\partial z_{iy}} \end{bmatrix} = \begin{bmatrix} \frac{g_+(|\vec{z}_i|)}{|\vec{z}_i|} + \frac{g'_+(|\vec{z}_i|)z_{ix}^2}{|\vec{z}_i|^2} - \frac{z_{ix}^2 g_+(|\vec{z}_i|)}{|\vec{z}_i|^3} & \frac{g'_+(|\vec{z}_i|)z_{ix}z_{iy}}{|\vec{z}_i|^2} - \frac{g_+(|\vec{z}_i|)z_{ix}z_{iy}}{|\vec{z}_i|^3} \\ \frac{g'_+(|\vec{z}_i|)z_{ix}z_{iy}}{|\vec{z}_i|^2} - \frac{g_+(|\vec{z}_i|)z_{ix}z_{iy}}{|\vec{z}_i|^3} & \frac{g_+(|\vec{z}_i|)}{|\vec{z}_i|} + \frac{g'_+(|\vec{z}_i|)z_{iy}^2}{|\vec{z}_i|^2} - \frac{z_{iy}^2 g_+(|\vec{z}_i|)}{|\vec{z}_i|^3} \end{bmatrix}. \tag{98}$$

Evaluating J at steady state $\vec{z}_i = \vec{z}_i^s$ simplifies the matrix considerably, due to the judicious choice of coordinate system aligned with the axis of the school. Specifically, since

$$\vec{z}_i^s = (z_{ix},\, z_{iy})^s = (d\,,\, 0), \tag{99}$$

substituting $z_{ix} = |\vec{z}_i| = d$, $z_{iy} = 0$ into (98) yields

$$Df \equiv \left(\frac{\partial \vec{f}_i}{\partial \vec{z}_i} |_{\vec{z}_i = \vec{z}_i^s} \right) = \begin{bmatrix} g'_+(d) & 0 \\ 0 & g_+(d)/d \end{bmatrix}.$$

Next, we write Eqs. (82)–(85) in matrix form as

$$\frac{\mathrm{d}}{\mathrm{d}t} \begin{bmatrix} \vec{\delta}_1 \\ \vec{\delta}_2 \\ \vdots \\ \vec{\delta}_n \\ \vec{\omega}_1 \\ \vec{\omega}_2 \\ \vdots \\ \vec{\omega}_n \end{bmatrix} = \left[\begin{array}{ccc|ccc} & 0 & & & I & \\ -- & -- & -- & -- & -- & -- \\ & D & & & -\gamma I & \end{array}\right] \begin{bmatrix} \vec{\delta}_1 \\ \vec{\delta}_2 \\ \vdots \\ \vec{\delta}_n \\ \vec{\omega}_1 \\ \vec{\omega}_2 \\ \vdots \\ \vec{\omega}_n \end{bmatrix}, \tag{100}$$

where

$$D = \begin{bmatrix} 0 & 0 & 0 & \dots & 0 & 0 \\ Df & -Df & 0 & \dots & 0 & 0 \\ 0 & Df & -Df & 0 & \dots & 0 \\ & & \vdots & & & \\ 0 & 0 & \dots & 0 & Df & -Df \end{bmatrix}, \tag{101}$$

where each 0 in the matrix represents a 2×2 matrix of zeros. D is a bidiagonal block matrix. We obtain the stability conditions by evaluating the eigenvalues of the coefficient matrix in Eq. (100) and determining under what conditions these eigenvalues have negative real part.

To find the eigenvalues of the coefficient matrix in Eq. (100), we form the determinant equation given by this coefficient matrix:

$$\det \begin{bmatrix} -\lambda I & I \\ D & -(\lambda + \gamma)I \end{bmatrix} = 0.$$

Next, we use the block matrix property from [18] introduced in Eq. (53). Noting that $-\lambda I$ and I commute, we have

$$\det \begin{bmatrix} -\lambda I & I \\ D & -(\lambda + \gamma)I \end{bmatrix} = \det\left(\lambda(\gamma + \lambda)I - D\right).$$

Recalling the definition of D in (101), where

$$Df = \begin{bmatrix} g'_+(d) & 0 \\ 0 & g_+(d)/d \end{bmatrix},$$

it is clear that D is a lower triangular matrix, and thus $(\lambda(\gamma+\lambda)I - D)$ is also a lower triangular matrix. $\lambda(\gamma+\lambda)$ appears in the first two diagonal entries (since each D entry is 2×2), while the remaining $2(n-1)$ diagonal entries contain $n-1$ pairs

$$\lambda(\gamma+\lambda) - g'_+(d),$$
$$\lambda(\gamma+\lambda) - g_+(d)/d.$$

The lower triangular structure allows us to immediately infer the eigenvalue equation, given by the product of diagonal terms, i.e.,

$$\left(\lambda(\gamma+\lambda)^2\right)\left(\lambda(\gamma+\lambda) - g'_+(d)\right)^{n-1}\left(\lambda(\gamma+\lambda) - g_+(d)/d\right)^{n-1} = 0.$$

We thus get solutions

$$\lambda = 0$$

with multiplicity 2,

$$\lambda = -\gamma$$

with multiplicity 2,

$$\lambda = -\frac{\gamma}{2} \pm \frac{\sqrt{\gamma^2 - 4g'_+(d)}}{2},$$

each with multiplicity $n-1$, and

$$\lambda = -\frac{\gamma}{2} \pm \frac{\sqrt{\gamma^2 - 4g_+(d)/d}}{2}$$

each with multiplicity $n-1$.

References

[1] I.D. Couzin, J. Krause, R. James, G.D. Ruxton, N.R. Franks, Collective memory and spatial sorting in animal groups, J. Theoret. Biol. 218 (2002) 1–11.
[2] A. Czirók, M. Vicsek, T. Vicsek, Collective motion of organisms in three dimensions, Physica A 264 (1999) 299–304.
[3] A. Czirók, T. Vicsek, Collective behaviour of interacting self-propelled particles, Physica A 281 (2000) 17–29.
[4] M.R. D'Orsogna, Y.L. Chuang, A.L. Bertozzi, L.S. Chayes, Self-propelled particles with soft-core interactions: Patterns, stability, and collapse, Phys. Rev. Lett. 96 (2006) 104302.
[5] A. Huth, C. Wissel, The simulation of movement of fish schools, J. Theoret. Biol. 156 (1992) 365–385.
[6] A. Huth, C. Wissel, The simulation of fish schools in comparison with experimental data, Ecol. Model. 75/76 (1994) 135–145.
[7] Y.L. Chuang, M.R. D'Orsogna, D. Marthaler, A.L. Bertozzi, L.S. Chayes, State transitions and the continuum limit for a 2d interacting, self-propelled particle system, Physica D 232 (2007) 33–47.
[8] H. Levine, W.J. Rappel, I. Cohen, Self-organization in systems of self-propelled particles, Phys. Rev. E 63 (2000) 017101.
[9] Y.-X. Li, Clustering in neural networks with heterogeneous and asymmetrical coupling strengths, Physica D 80 (3) (2003) 210–234.
[10] R. Lukeman, Y.-X. Li, L. Edelstein-Keshet, A mathematical model for milling formations in biological aggregates, Bull. Math. Biol. (2007) (submitted for publication).
[11] A. Mogilner, L. Edelstein-Keshet, L. Bent, A. Spiros, Mutual interactions, potentials, and individual distance in a social aggregation, J. Math. Biol. 47 (2003) 353–389.
[12] H.-S. Niwa, Self-organizing dynamic model of fish schooling, J. Theoret. Biol. 171 (1994) 123–136.
[13] H.-S. Niwa, Newtonian dynamical approach to fish schooling, J. Theoret. Biol. 181 (1996) 47–63.
[14] H.-S. Niwa, Migration of fish schools in heterothermal environments, J Theor. Biolet. 193 (1998) 215–231.
[15] A. Okubo, Diffusion and ecological problems: Mathematical models, Springer Verlag, New York, 1980.
[16] A. Okubo, D. Grunbaum, L. Edelstein-Keshet, The dynamics of animal grouping, in: A. Okubo, S. Levin (Eds.), Diffusion and Ecological Problems: Modern Perspectives, Springer, New York, 2001.
[17] S. Sakai, A model for group structure and its behavior, Biophys. Japan 13 (1973) 82–90.
[18] J.R. Silvester, Determinants of block matrices, Math. Gaz. 84 (2000) 460–467.
[19] A.R.E. Sinclair, The African buffalo: A study of resource limitation of populations, University of Chicago Press, Chicago, 1977.
[20] R. Suzuki, S. Sakai, Movement of a group of animals, Biophys. Japan 13 (1973) 281–282.
[21] J. Toner, Y. Tu, Long-range order in a two-dimensional xy model: How birds fly together, Phys. Rev. Lett. 75 (23) (1995) 4326–4329.
[22] C. Topaz, A. Bertozzi, Swarming patterns in a two-dimensional kinematic model for biological groups, SIAM J. Appl. Math. 65 (1) (2004) 152–174.
[23] C. Topaz, A. Bertozzi, M. Lewis, A nonlocal continuum model for biological aggregation, Bull. Math. Biol. 68 (7) (2006) 1601–1623.
[24] B.P. Uvarov, Locusts and grasshoppers, Imperial Bureau of Entomology, London, 1928.
[25] T. Vicsek, A. Czirók, E. Ben-Jacob, I. Cohen, O. Shochet, Novel type of phase transition in a system of self-driven particles, Phys. Rev. Lett. 75 (6) (1995) 1226–1229.
[26] D. Weihs, Energetic advantages of burst swimming of fish, J. Theoret. Biol. 48 (1974) 215–229.